Challenges and Strategies for Optimizing Corrosion and Biodegradation Stability of Biomedical Micro- and Nanoswimmers

A Review

Rahimi, Ehsan; Sanchis-Gual, Roger; Chen, Xiangzhong; Imani, Amin; Gonzalez-Garcia, Yaiza; Asselin, Edouard; Mol, Arjan; Fedrizzi, Lorenzo; Pané, Salvador; Lekka, Maria

DOI
10.1002/adfm.202210345

Publication date
2023

Document Version
Final published version

Published in
Advanced Functional Materials

Citation (APA)
Rahimi, E., Sanchis-Gual, R., Chen, X., Imani, A., Gonzalez-Garcia, Y., Asselin, E., Mol, A., Fedrizzi, L., Pané, S., & Lekka, M. (2023). Challenges and Strategies for Optimizing Corrosion and Biodegradation Stability of Biomedical Micro- and Nanoswimmers: A Review. *Advanced Functional Materials*, *33*(44), Article 2210345. https://doi.org/10.1002/adfm.202210345

ADVANCED FUNCTIONAL MATERIALS
www.afm-journal.de

Challenges and Strategies for Optimizing Corrosion and Biodegradation Stability of Biomedical Micro- and Nanoswimmers: A Review

Ehsan Rahimi, Roger Sanchis-Gual,* Xiangzhong Chen, Amin Imani, Yaiza Gonzalez-Garcia, Edouard Asselin, Arjan Mol, Lorenzo Fedrizzi, Salvador Pané, and Maria Lekka**

The last two decades have witnessed the emergence of micro- and nanoswimmers (MNSs). Researchers have invested significant efforts in engineering motile micro- and nanodevices to address current limitations in minimally invasive medicine. MNSs can move through complex fluid media by using chemical fuels or external energy sources such as magnetic fields, ultrasound, or light. Despite significant advancements in their locomotion and functionalities, the gradual deterioration of MNSs in human physiological media is often overlooked. Corrosion and biodegradation caused by chemical reactions with surrounding medium and the activity of biological agents can significantly affect their chemical stability and functional properties during their lifetime performance. It is therefore essential to understand the degradation mechanisms and factors that influence them to design ideal biomedical MNSs that are affordable, highly efficient, and sufficiently resistant to degradation (at least during their service time). This review summarizes recent studies that delve into the physicochemical characteristics and complex environmental factors affecting the corrosion and biodegradation of MNSs, with a focus on metal-based devices. Additionally, different strategies are discussed to enhance and/or optimize their stability. Conversely, controlled degradation of non-toxic MNSs can be highly advantageous for numerous biomedical applications, allowing for less invasive, safer, and more efficient treatments.

1. Introduction

Biomedical micro- and nanoswimmers (MNSs) are being intensively explored for their potential to address challenges in medical procedures, including targeted drug delivery, nanosurgery, localized biopsy, cell storage, and isolation of biological targets.[1–4] To achieve optimal performance, a biomedical small-scale swimmer should be engineered with several key features, including motion capabilities, precise control, the ability to release therapeutic payloads at targeted sites, and biocompatibility.[5–10] The motion capabilities of these devices in the human physiological environment are key for accessing hard-to-reach areas. These small-scale devices require a driving force[11] to move, which can be provided by surrounding available fuels (chemical propulsion) or external energy sources. The type of propulsion is significantly dependent on the swimmer's material properties. For example, chemically propelled swimmers must comprise a surface

E. Rahimi, L. Fedrizzi
Polytechnic Department of Engineering and Architecture
University of Udine
33100 Udine, Italy
E-mail: e.rahimi-2@tudelft.nl

E. Rahimi, Y. Gonzalez-Garcia, A. Mol
Delft University of Technology
Department of Materials Science and Engineering
Mekelweg 2, 2628 CD Delft, The Netherlands

R. Sanchis-Gual, X. Chen, S. Pané
Multi-Scale Robotics Lab (MSRL)
Institute of Robotics & Intelligent Systems (IRIS)
ETH Zurich
8092 Zurich, Switzerland
E-mail: rsanchis@ethz.ch

A. Imani, E. Asselin
Department of Materials Engineering
The University of British Columbia
Vancouver, BC V6T 1Z4, Canada

M. Lekka
CIDETEC
Basque Research and Technology Alliance (BRTA)
Donostia, 20014 San Sebastián, Spain
E-mail: mlekka@cidetec.es

The ORCID identification number(s) for the author(s) of this article can be found under https://doi.org/10.1002/adfm.202210345

DOI: 10.1002/adfm.202210345

that is chemically active.[11–13] The vast majority of these are composed of a catalyst that increases the transformation rate of a chemical compound present in the swimming media. Some of these swimmers can also comprise a sacrificial building block that reacts with a substance of the environment.[14] Note that, for this specific type of chemical swimmers, an accelerated corrosion might be desirable for their fast propulsion. Chemically propelled swimmers are motors (and not robotic systems) because their speed and trajectory cannot be controlled. When the swimmer's motion is controlled by an external source of energy, such as electrical or magnetic fields, ultrasound, light, or combinations thereof, they are considered small-scale robots because their speed, directionality (and, in some occasions, the locomotion mechanism), can be externally controlled by tuning the energy of the source.[5,15,16]

While many strategies have been explored to optimize the functional properties of MNSs by varying their structure, shape and size,[11] chemical composition,[14] complexity,[17,18] and surface properties (thin film coatings[19] and/or organic functionalization[20,21]), properties such as durability and corrosion resistance are often overlooked despite their importance in ensuring an optimal functionality.[22] Several MNSs' designs comprise one or more metallic components that can easily degrade, compromising their motion performance and functionalities. Furthermore, the degradation of these materials can release toxic metal ions that can harm cells and tissues.[5] Corrosion and biodegradation depend on the material and the working environment. The human body is a harsh environment for many materials, especially metals, due to the presence of aggressive ions such as Cl^- and F^-, reactive oxygen species (ROS) such as H_2O_2 and $OH^•$, weakly formed calcium phosphate films,[23] the possibility of the Fenton reaction between iron ions and hydrogen peroxide,[24] and the coordination of proteins and diverse macrophages/cell species.[25,26] Corrosion is a significant issue for miniaturized devices, as they can degrade in shorter times, leading to the premature loss of their functionality. Corrosion phenomena in micro- and nanodimensional components can develop differently than in their bulk counterparts, and the integration of several materials in physical contact can result in galvanic coupling, where the less noble material corrodes or dissolves entirely due to its smaller size and high electrochemically active (less protective surface area). Different metals and their alloys exhibit varying rates and mechanisms of degradation. Metals such as Fe, Mg, and Zn usually experience rapid degradation, while metals with passivity behavior such as Ni, Co, and Ti exhibit slow deterioration due to the presence of a protective passive film.[27–29] In contrast, noble metals like Au and Pt are, in principle, inert.[25] Degradation can lead to the loss of stimuli-responsive abilities and mechanical properties of MNSs, impairing their swimming performance.[17,22,30] However, some MNSs have shown to preserve their functionality for a certain amount of time in in vitro or in vivo environments without adverse effects from released metal ions.[31] For biomedical applications, the safe decomposition of MNSs once their tasks are accomplished is of interest to avoid bioaccumulation in tissues.[32–35] In this regard, some reviews have already discussed the latest advances in the preparation and application of biodegradable MNSs.[36–38] Yet, a mechanistic understanding of the corrosion and biodegradation processes in physiological environments and biological species is necessary to design MNSs with appropriate degradation rates.

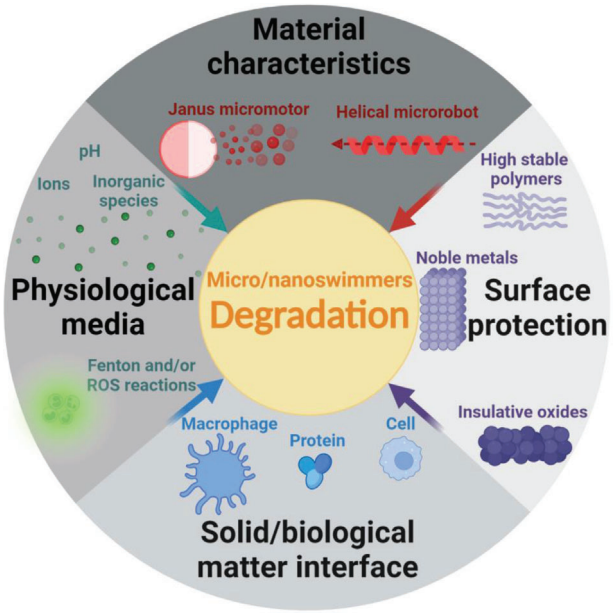

Figure 1. Schematic representation of the review outline. Four main features, including material characteristics, physiological media, solid/biological matter interface, and surface protection influence the degradation process of biomedical micro/nanoswimmers.

This review explores the influence of material characteristics, environmental conditions, and types of interfaces on the corrosion and biodegradation behaviors and functional properties of metallic and metal oxide-based MNSs in different parts of the human body. The text also discusses surface protection methods based on thin films that can improve corrosion and biodegradation resistance and the long-term durability of MNSs. **Figure 1** summarizes the relationships between the corrosion and biodegradation resistance, functional properties, and specific nature of solid/liquid interfaces that can affect the short- or long-term performance of MNSs.

2. Corrosion and Biodegradation Processes in Micro and Nanoswimmers

2.1. Corrosion and Biodegradation Mechanisms

MNSs are prone to corrosion and deterioration after prolonged immersion in human physiological media. The corrosion and biodegradation processes of metallic and oxide biomaterials, such as surgical implants and MNSs, are complex and are influenced by changes in pH, biological fluids, exposure to cellular processes, and the chemical environment within the body.[23,39] **Figure 2** provides a graphical summary of the various corrosion and biodegradation events:

a) Galvanic coupling occurs due to different metal nobilities (or work function (WF)), leading to the creation of two separate regions - an anodic zone (Zn or Mg) with accelerated metal ion release and a cathodic zone (Pt or Au) supporting

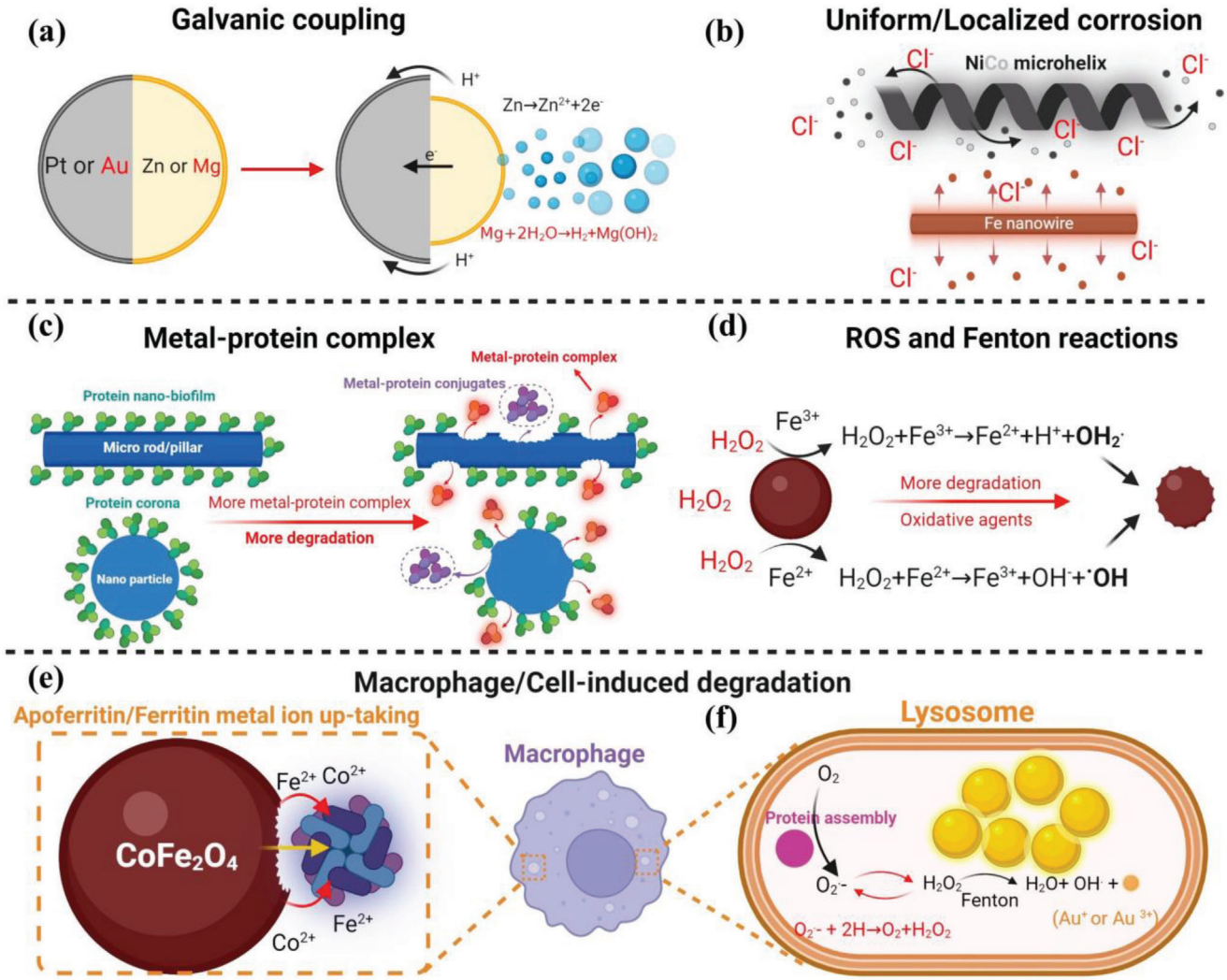

Figure 2. Summarized schematic representation of the corrosion and biodegradation processes on the surface of biomedical micro- or nanoswimmers. a) Galvanic coupling. b) Uniform/localized corrosion. c) Metal-protein complex. d) ROS and Fenton reactions. e,f) Macrophage/cell-induced degradation. f) has been re-sketched and adapted with permission.[43] Copyright 2020, National Academy of Sciences.

reduction reactions (e.g., hydrogen generation or oxygen reduction).

b) Uniform corrosion occurs when the entire exposed material surface undergoes metal ion release owing to its high electrochemical activity, with no preferential dissolution of different parts (e.g., the nanoparticle or nanowire of iron/iron oxide). However, localized corrosion and biodegradation on MNSs strongly depend on the local chemical heterogeneity and/or specific location on MNS surfaces. For example, NiCo alloy-based microswimmers can create a local preferential dissolution of Co compared to Ni, causing pitting corrosion or high energy sites for electrochemical activities that can be located on the edge, kink, and grain boundaries of the MNSs chassis.[22]

c) Formation and subsequent stabilization of protein nanobiofilm on the surface of microswimmers (micropillar) or nanoparticles (protein thin films, termed protein corona) after a short or long immersion can accelerate the biodegradation or metal ion release due to the detachment of metal-bound proteins into metal-protein complexes or metal-protein conjugates.[22,25]

d) ROS can impair the chemical stability of MNSs. In particular, Fenton reactions occur due to the chemical interaction of released Fe^{2+} and Fe^{3+} from iron/iron oxide MNSs with ROS, leading to the production of oxidative agents ($OH_2\cdot$ and $\cdot OH$),[31,40,41] which eventually causes enhanced degradation.

e) Biodegradation of ceramic oxide nanoparticles inside liver lysosomes or spleen macrophages is due to the adsorption of apoferritin or ferritin protein molecules on the nanoparticle surface and the initiation of the deterioration process upon metal-protein complex formation and metal ion uptake.[42]

f) Unstable radicals produced by membrane protein assemblies based on spontaneous dismutation or via superoxide dismutase (SOD) reactions cause the production of O_2 and H_2O_2. The interaction of H_2O_2 with metals (e.g., gold nanoparticles)

produces an oxidized metal that can trigger the formation of ionic metallic ions.[43]

2.2. Corrosion and Biodegradation Monitoring

To better understand the degradation mechanisms of MNSs and improve their stability, it is essential to investigate corrosion and biodegradation mechanisms. However, only limited studies on the subject have been conducted so far.[17,30,44] To gain insights into these processes and design ideal MNSs with optimized stability, various techniques can be employed.

1) Ex-situ methods, including morphological and surface chemical analyses through scanning electron microscopy (SEM),[22] Transmission electron microscopy (TEM),[45] and energy-dispersive X-ray spectroscopy (EDXS),[46] have been utilized to observe corrosion and biodegradation after immersion in corrosive media for a certain period of time.[30,44] SEM and TEM can provide valuable information on MNS morphology changes, while EDXS shows atomic percentage variations during the degradation process.
2) Chemical analyses of the corrosive media via inductively coupled plasma atomic emission spectroscopy (ICP-AES) or inductively coupled plasma mass spectrometry (ICP-MS) have been used to measure the evolution of metallic concentrations in the media over time and monitor metal ion release from the MNS.[17,30] A detailed discussion of these techniques may be found in.[47]
3) Electrochemical measurements, such as open circuit potential (OCP), potentiodynamic polarization (PDP), and electrochemical impedance spectroscopy (EIS), can provide specific insights into MNS degradation.[22] These techniques can predict how metallic materials will participate in electrochemical corrosion reactions in a given medium (further details can be found in[48]). Such measurements are particularly useful for evaluating the kinetics of corrosion and the efficiency of protective layers on MNS.
4) Indirect methods for detecting MNS performance deterioration (e.g., magnetization response [22] or local surface plasmon resonance (LSPR)[44]) have also been used to estimate their useful lifespan.

3. Factors Influencing the Corrosion and Biodegradation of Micro and Nanoswimmers

Overall, biomedical MNSs require several critical features to function effectively in the human body. These properties include biocompatibility, resistance to metal ion release and biodegradation, non-toxicity of released materials in vivo, positive host response, easy manipulation, precise control, and release of embedded functional cargoes to targeted sites. However, achieving all of these complex functionalities in a single miniature device is challenging, and several factors must be considered, such as corrosion behavior and biodegradation mechanisms. Moreover, as the miniature devices travel to the desired site, they encounter various complex biological environments, which have varying impacts on their corrosion and biodegradation behaviors. As illustrated in Figure 1, the corrosion and biodegradation resistance behavior and functional properties of MNSs strongly depend on the material characteristics, the specific nature of solid/liquid interfaces, and the properties of physiological media with different types of biological species that can affect the short- and/or long-term corrosion and biodegradation resistance of the MNS. Therefore, it is crucial to carefully consider these factors to develop effective biomedical MNSs that can perform their intended functions safely and reliably within the human body.

3.1. Material and Design Characteristics

3.1.1. Shape, Size, and Configuration

Miniaturization of devices can result in accelerated device degradation and corrosion due to the higher concentration of surface atoms as devices become smaller. Additionally, while there are several facile manufacturing approaches that can produce MNSs with custom shapes and sizes at a low cost (**Figure 3**), these methods may also result in structures with a greater number of surface defects and non-uniformity, which can have detrimental effects on the MNSs' durability.[11,22,49]

Due to miniaturization, small-scale devices can also be more susceptible to corrosion during their actuation. For example, studies on helical propellers made of SiO_2/Co have found that decreasing the helix length to less than 1 μm requires a substantially higher operating frequency of the rotating magnetic field to efficiently control the device.[50] In these conditions, smaller cobalt helical propellers may be more susceptible to corrosion and biodegradation processes. The increase in rotational velocity can enhance the mass transfer rate of corrosive species near the swimmer's surface and hinder the formation of protective oxide layers.

The arrangement of the components within a swimmer can also have a significant impact on its ability to resist corrosion. For instance, multi-metallic nanoswimmers, such as the wire-based nanorobot described in,[51] comprise alternating segments of nickel (for magnetic actuation), silver (as flexible hinges), and gold (for structural support). Note that these metal segments display different WFs, and, subsequently, are highly susceptible to display galvanic coupling (Figure 3E), which can lead to the acceleration of oxidative reactions or dissolution in the active region (where the electrochemical activity is high).

3.1.2. Chemical Composition

To date, we can find a wealth of MNSs made of different materials, including inert metals (e.g., Au,[52] Ru,[53] Rh,[54] Pt,[55] Ag,[56] and Ga[57]), biodegradable metals (e.g., Fe,[58] Zn,[59] and Mg[60]), metals prone to passivate (e.g., Ti,[61] Ni,[62] Co,[63] and Cu[64]), and metal oxides (e.g., Fe_xO_y,[20,65] MnO_2,[66] SiO_2,[67] $CoFe_2O_4$,[21,68] and $NiFe_2O_4$[69]) (**Table 1**). Note that the release of metal ions can be expected over time in all the above-mentioned materials to a different extent, including oxide ceramics, which are often perceived as very stable but may still undergo gradual biodegradation and release of metal ions in physiological environments.[42] Hence, the chemical stability and resistance to metal ion release of MNSs must be carefully considered when

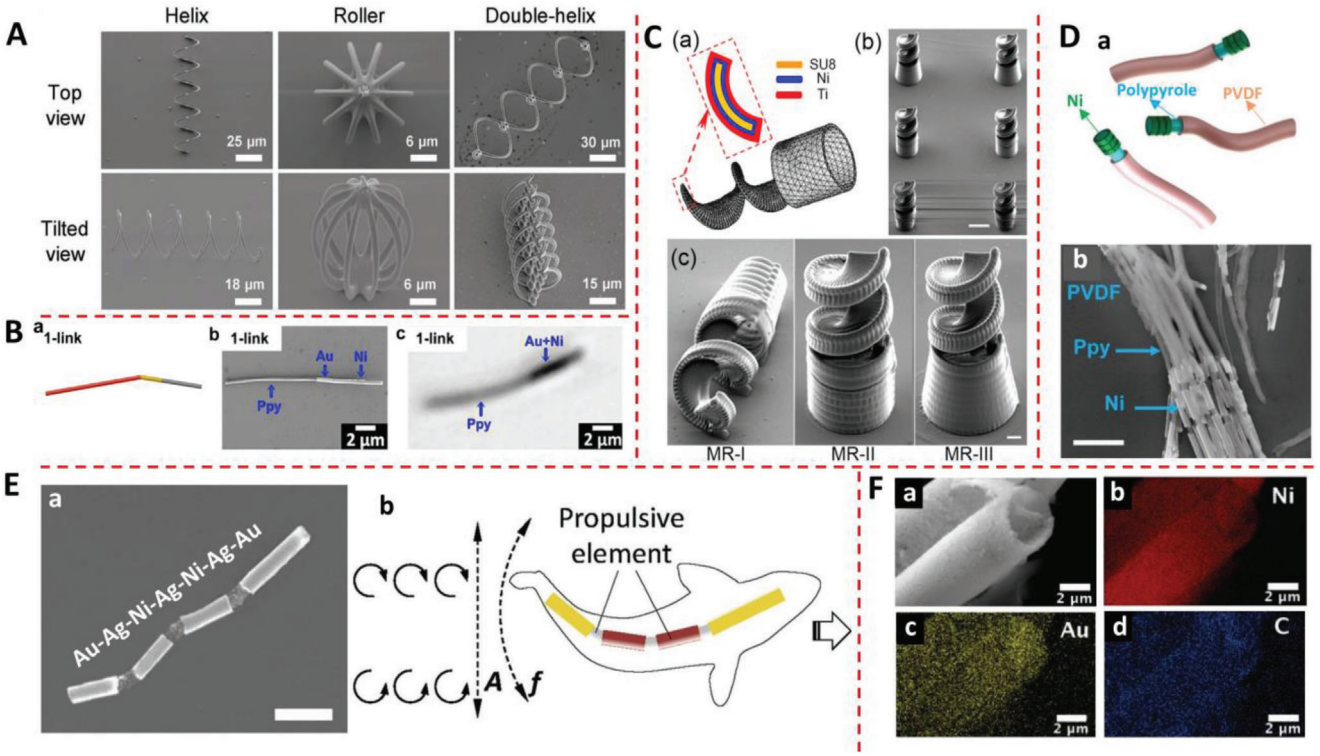

Figure 3. A) Top view and tilted view SEM images of iron microhelices and microrollers fabricated by 3D-assissted electrodeposition. Adapted with permission.[58] Copyright 2019, Wiley-VCH GmbH. B) (a–c) Schematic representation, SEM and optical images of Ni/Au/Ppy3-link swimmers, respectively. Adapted with permission. [183] Copyright 2015, American Chemical Society. C) (a) Fabrication of microrobots utilizing SU8 photoresist followed by coating them with a thin Ni/Ti bilayer. (b,c) SEM images of microrobots with different head design. Scale bars correspond to 10 and 2 μm, respectively. Adapted with permission.[184] Copyright 2014, American Institute of Physics. D) (a) Schematic representation and (b) SEM image of magnetic nanoeels (Ni/polyvinylidene fluoride (PVDF)/polypyrole). The scale bar corresponds to 2 μm. Adapted with permission.[76] Copyright 2019, Wiley-VCH GmbH. E) (a) SEM image of a multilinked artificial nanofish made by electrodeposition. Scale bar: 800 nm. (b) Schematic illustration of an artificial nanofish in body and caudal fin mode propulsion, involving passing undulatory waves down the entire length of the body. Adapted with permission.[51] Copyright 2016, Wiley-VCH GmbH. F) (a–d) SEM and EDXS elemental maps of Ni/Au/chitosan nanotube. Adapted with permission.[75] Copyright 2016, The Royal Society of Chemistry.

selecting their composition to avoid adverse effects on biocompatibility and toxicity,[5,70] which can ultimately lead to detrimental effects on the human immune system.[71] Additionally, even if a material appears inert in a certain environment, electrochemical interactions can also occur on its surface, triggering the denaturation of proteins and tissues upon contact.[26]

The corrosion and biodegradation resistances, and biocompatibility of metallic MNSs, whether fully or partially passive, are closely linked to their ability to form a dense, adherent oxide surface layer, typically with thickness in the range of 2–10 nm, which is maintained during in vivo exposure.[72,73] While protective corrosion was not a primary design consideration, there are examples of MNSs that could possess these characteristics, including Al-Ga/Ti,[74] CoNiReP,[63] Ni/Au,[75] and Ni/Ppy (polypyrrole)/PVDF.[76] The distinguishing features of simple or complex oxide films on passive-metallic MNSs and their relative stability can impede electron and metal ion transfer at the electrolyte/solid interface.[77] However, over time, the protective passive film can experience a slow release of metal ions and become severely damaged or chemically degraded (passive film breakdown) under particularly harsh conditions.[78] The compact oxide film on passive-metallic MNSs is susceptible to destruction or dissolution rates, particularly in the presence of aggressive ions such as Cl^-.[79] The likelihood of pitting corrosion attacks on passive-metallic MNSs increases with the concentration of aggressive ions, a lower pH, and the presence of biological substances such as proteins, cells, and ROS.[80,81]

The susceptibility of metallic MNSs to galvanic corrosion and dealloying is a significant concern since many MNS designs comprise at least two metals. Galvanic corrosion occurs when two dissimilar metals or alloys are electrically connected, leading to the establishment of two separate regions with different corrosion rates.[80] The anodic region, where the corrosion reaction rate is higher, is at the active site, while the cathodic region, where the reaction rate is lower, is at the noble site. When small-scale swimmers made up of different metal segments or coated with other metals or alloys, come into contact, a strong galvanic coupling between them can be established, even through micro- or nanodefects within the protective layer.[22] Furthermore, the electronic surface properties of the material play a significant role in electrochemical interactions.[82,83] Studies suggest that materials with high surface potential or WF (Φ) values have higher stability of valence electrons or a more stable electronic state, which restricts their participation in electrochemical reactions. Therefore,

Table 1. The various types of MNSs with different chemical compositions and corrosion/biodegradation mechanisms. The proposed corrosion mechanism is based on the work function of metals and oxides,[87,88] and the electromotive force of oxidation-reduction reactions.[80].

Shape and size	Chemical composition	Mechanism of motion	Application	Solution, pH and T	Targeting ability	Degradation time	Corrosion/biodegradation mechanism	Ref
Microtubular	PANI/Zn	Hydrogen- bubble propelled	Biomedical	HCl,−0.2 - 1 and room temperature	Highest and lowest velocity at pH −0.2 and 1	-	Uniform corrosion (Zn anodic site)	[117]
Microtubular	PEDOT/MnO_2/Ag	Hydrogen- bubble propelled	Anti-bacterial	0.2–5% H_2O_2 and room temperature	-	-	Localized/Galvanic corrosion (Ag anodic side)	[185]
Janus microball	Al-Ga/Ti	Hydrogen- bubble propelled	Biomedical	PBS, 7 and room temperature	-	-	Localized/Galvanic corrosion (Al anodic side)	[74]
Janus microball	Mg/Pt	Hydrogen- bubble propelled	Biomedical	PBS + 0.5mN$aHCO_3$ and 5 wt% PVP	-	70 s (Average value)	Localized/Galvanic corrosion (Mg anodic side)	[60]
Microhelix/roller	Fe	External magnetic field	Biomedical	RPMI 1640 Medium,7.4 and room temperature	2–4 days (captured cancer cell)	-	Uniform corrosion	[58]
Janus microball	Zn/Pt	Hydrogen- bubble propelled	Biomedical	Culture medium and room temperature	30 min (lowest content of E.*coli* cell)	-	Galvanic corrosion (Zn anodic side)	[59]
Microtubular	Bi/Ni/Pt	External magnetic field	Drug delivery	0.5% SDS + 1%H_2O_2, 37 °C	60 min (highest removal of heavy metals)	-	Galvanic corrosion (Ni anodic side)	[186]
Microparticles	Ag and MnO_2	H_2O_2 decomposition-propelled	Biomedical	0.1–12% H_2O_2 and 23 °C	-	-	Uniform corrosion	[66]
Janus microball	SiO_2/Pt	H_2O_2 decomposition-propelled	Biomedical	0–10% H_2O_2 and 23 °C	-	-	Localized corrosion	[67]
Micro tubular and helical	CoNiReP	External magnetic field	Biomedical	-	-	-	Galvanic corrosion (more anodic in Co and Re sites [87])	[63]
Micro and nanotubular	Pt	H_2O_2 decomposition-propelled	Biomedical	0–10% H_2O_2 and 23 °C	Lowest and highest velocities at 0 and 10% H_2O_2	-	Localized corrosion/Uniform corrosion	[187]

(*Continued*)

Table 1. (Continued).

Shape and size	Chemical composition	Mechanism of motion	Application	Solution, pH and T	Targeting ability	Degradation time	Corrosion/biodegradation mechanism	Ref
Nanotube	Ni/Chi/Au	External magnetic field	Drug delivery	PBS, 6 –7.4 and room temperature	Drug release after 24 h (pH 7.4) and 48 h (pH 6.8)	-	Galvanic corrosion (Ni anodic side)	[75]
Nanowire	Fe/C	External magnetic field	Drug delivery	Water and room temperature	-	-	Localized/Galvanic corrosion (Fe anodic side)	[188]
Nanowire	Co/Au	External magnetic field	Biomedical	-	-	-	Galvanic corrosion (Co anodic side)	[189]
Nanowire	Ni/Ppy/P	External magnetic field	Drug delivery	Tris HCl, pH 8.5 and room temperature	Highest drug delivery at 90 min	-	Uniform corrosion of Ni	[76]
Nanoparticles	Fe	External magnetic field	Cancer theranostics	Buffer media, 7.4, 6.5, 5.4, and 37 °C	Lowest cell viability at pH 6.5 after 24 h	Completely dissolve at pH 6.5 after 48 h	Uniform corrosion	[24]
Nanoparticles	Fe/PEG	External magnetic field	Biomedical	PBS and 37 °C	Lowest uptake of NPs by cells after 4 h	-	Uniform corrosion of Fe	[175]
Nanoparticles	Fe/Gd_2O_3	External magnetic field	Biomedical	PBS and 37 °C	Lowest cell viability after 48 h	-	Localized/Galvanic corrosion (Fe anodic side)	[125]
Nanoparticles	Fe/Chi, PEG or PEI	External magnetic field	Cancer therapy	Buffer media and 37 °C	Lowest Clonogenic survival after 3 days	-	Localized corrosion (Fe anodic side)	[190]
Nanoparticles	Fe/Au	External magnetic field	Hepatoma imaging	-	-	-	Localized/Galvanic corrosion (Fe anodic side)	[191]
Nanoparticles	CFO and NFO	External magnetic field	Biomedical	Cell culture medium and 37 °C	Inhibit the cell division by 2 g L^{-1} of CFO	CFO: Co^{2+} 200 ppb, NFO: Ni^{2+} 120 ppb after 24 h	Uniform corrosion	[69]
Nanoparticles	Ag/Au	External laser (Photothermal)	Photothermal Therapy	PBS and 37 °C	High photothermal efficiency after 25 days	Ag completely dissolved after 25 days	Galvanic corrosion (Ag anodic side)	[192]

materials with high WF values exhibit higher electrochemical nobility and may be considered a criterion for predicting corrosion behavior.[84,85]

Previous studies on various types of bimetallic MNSs, such as Pt-Cu microrods,[64] Au-Ni-Au microwires,[86] Au/B-TiO_2 Janus micromotors, Ag-Pt nanorods,[56] and Ni-Au-PPy nanorods,[62] have shown that both Au and Pt elements inherently have a higher WF than other coupled metals such as Cu, Ag, Ni, Ti, and Fe. The WF values of Au and Pt are Φ_{Au} = 5.31 eV and Φ_{Pt} = 5.65 eV, respectively, which are important criteria for predicting the corrosion behavior of metallic MNSs.[87] Passive metals tend to form oxide layers rapidly when exposed to air or an electrolyte, which increases the WF of their oxide compared to their pure metal state.[88] However, these passive films have various atomic defects and are highly susceptible to pitting or other localized degradation caused by corrosive ions and biological substances in the human body.[89] Therefore, two distinct sites of bimetallic MNSs can be distinguished: a) cathodic or noble regions (Au and Pt), which support enhanced reduction processes, and b) anodic or active regions (Cu, Ag, Ni, Ti, and Fe), which display a high tendency to release metal ions. Moreover, internal galvanic coupling can also occur between various phases of composite MNSs.[22,85,90] Note that the dynamic conditions of the human body and the presence of various biological substances can cause the passive electrochemical potential of metallic MNSs to shift toward a more positive value, which subsequently increases localized corrosion on the active site.[91] Consequently, metallic MNSs may gradually fail to achieve the desired swimming speed, efficiency, and controllability due to degradation at active component sites.

Propulsion is a crucial factor to consider in the development of micro- and nanoscale devices, as it directly influences their functionality and performance. For certain MNSs, their propulsion depends on their surface chemistry or chemical composition, posing significant challenges for producing ideal MNSs for specific applications. The surface chemistry of MNSs is essential for determining their power source, mechanical movement, target site, and mission duration, all of which can be influenced by corrosion and biodegradation events.[22,30] Corrosion and biodegradation are especially concerning for chemically powered MNSs, which rely on oxidation and reduction reactions on their surfaces that can lead to the release of metal ions and result in toxic effects.

Recent studies have shown that inducing accelerated corrosion of metals in physiological fluids can enhance the performance of micro- and nanomotors. For instance, Mg-based Janus micro- and nanomotors have been effectively deployed to treat gastric bacterial infections in the stomach.[32,92,93] The efficient propulsion of these micromotors in the stomach relies on the dissolution of the Mg layer in the highly acidic gastric juice (pH ~ 1–3) and the generation of hydrogen microbubbles. While there are examples of enzymatic propulsion, most external chemical fuels used for chemical swimmers are not biocompatible, raising concerns about their safety in biological media. Consequently, external power sources have become increasingly popular due to their adaptability and compatibility with biological environments.[94] Magnetic fields are a versatile source of propulsion for MNSs that can improve their functional properties and enable a wide range of locomotion mechanisms (Figure 3). However, magnetic MNSs made of Fe, Ni, and Co are prone to corrosion and biodegradation, requiring a careful material selection and design. To improve their lifespan and efficiency of magnetically propelled MNSs and ensure safe elimination from the human body, biocompatible materials and coatings must be considered. Therefore, careful consideration of the selection and design of materials is crucial to ensure that magnetically propelled MNSs can operate effectively in biological environments and avoid adverse effects on human health.

3.2. Surface Physical Properties

The surface physical properties of MNSs are crucial in determining their interactions at the solid/liquid interface. The physical properties of a solid surface, such as its electronic properties, surface charge, surface energy, wettability (hydrophobicity and hydrophilicity), and roughness/morphology distribution, all play important roles in influencing the behavior and properties of MNSs. These properties impact electrochemical/catalytic interactions, surface-dependent functional properties, swimming/locomotion type and speed, long-term durability or resistance to degradation processes, and biomolecular interactions that may result in biomolecular nanofilms.[95–98] For chemically propelled swimmers, the catalytic activity and electrochemical interactions depend on the effective surface area exposed to the fluid environment, which can be increased by surface patterning.[99,100] In particular, incorporating nanoscale features with diverse morphologies on the surface of self-propelled MNSs can result in a higher effective surface area and faster swimming speed.[101] However, although increasing the effective surface area provides benefits for improving the functional properties of MNSs, a larger accessible surface area also enables aggressive ions, proteins, and other biological species to interact with the swimmer's surface, thus resulting in corrosion, biodegradation, or other negative impacts.

Additionally, the crystallinity and microstructure distribution of MNSs with various shapes and sizes can also significantly influence the electrochemical interactions (particularly on self-propelled MNSs) on their surfaces and thus, their service time. Based on a previous study on the role of crystallinity in self-propelled MnO_2-based oxides with spherical microparticles, MnO_2 with different and intensive crystalline forms (polymorphism) exhibited a higher average speed than the low-polymorphic structure.[102] Therefore, a different lifetime is expected because of the different catalytic activity of the particles in contact with the fuel, which thereby modifies the rate of degradation.

In addition, the impacts of hydrophobicity and hydrophilicity on the motion speed of MNSs were investigated for nanoflask-propelled robots.[103] Results showed that the hydrophobic nanoflask robots moved at a relatively low speed (forward direction) compared with the hydrophilic nanoflask robots (backward direction), indicating that the increase in wettability decreases the resistance to corrosion and degradation.

The surface charge of MNSs is a crucial physical property that has a direct impact on various aspects of their behavior. It affects the adsorption of ions and biomolecules such as proteins, which can lead to detrimental effects such as corrosion and biodegradation caused by protein-metal complex formation and

detachment. The surface charge also influences redox reactions and can affect the performance of MNSs.[104,105] Self-electrophoretic catalytic MNSs utilize surface charge to facilitate the preferential reduction and oxidation of chemical agents, such as H_2O_2, at the cathodic (more noble) and anodic (more active) sites, respectively. This results in the creation of positive and negative regions at the ends of the MNS, establishing a self-generated electrical field, which ultimately induces motion and modifies the lifespan of the structure.[104,106]

3.3. Role of Physiological Media in Degradation Mechanisms

Human physiological media comprise various ions, organic and inorganic species such as chloride (Cl^-), sodium (Na^+), phosphate ($H_2PO_4^-$, HPO_4^{2-}), calcium (Ca^{2+}), magnesium (Mg^{2+}), potassium (K^+), sulfate and bicarbonate ions, proteins (albumin, fibronectin, globulin, etc), and cells, which can hinder or accelerate the degradation of metallic materials, depending on their characteristics.[23,107] A specific classification of the individual roles of these various species in the short- or long-term corrosion resistivity of these miniature devices in complex human body fluids is an essential topic that should be taken into consideration.

3.3.1. Ions, Inorganic Species, and pH

The ionic species play various functions in human biological fluids, such as regulating and maintaining the body's pH levels and participating in electrochemical and electron transfer reactions.[107] When biomaterials are implanted, the internal environment of the human body surrounding them is disturbed due to changes in blood supply and a shift in the ionic equilibrium.[107] However, from a corrosion perspective, some of these ionic species represent detrimental (Cl^-) or inhibitory (Ca^{+2} and phosphate) effects on the corrosion stability of metallic biomaterials.[108] Both Cl^- and F^- ions are aggressive ions, and their different concentrations can significantly impact the corrosion resistance behavior of metallic biomaterials.[109] The chemistry of blood plasma is extremely aggressive for a wide range of metallic biomaterials, particularly because of the high Cl^- concentration (0.9 wt% NaCl).[39,110] Therefore, in the case of passive-metallic biomaterials, Cl^- ions can easily penetrate the passive film, accumulate at the metal/passive film interface, and eventually undergo passive film breakdown.[79] The F^- ion is also an aggressive ion, similar to Cl^-, that can strongly reduce the corrosion resistivity of metallic biomaterials, which is a particularly detrimental synergistic effect of Cl^- ions.[111] As previously reported, the corrosion resistance of titanium decreases in solutions containing F^- ions (2 g L^{-1} at pH 5) due to acceleration in the formation of titanium fluoride complexes.[109] Notably, the inhomogeneous chemical composition of bulk and passive layers alongside chemical/physical heterogeneity at the surface, such as defects including steps, kinks, inclusions, dislocations, and grain boundaries with different angles and various mechanical damages, can facilitate the degradation of metallic biomaterials by aggressive ions.[80] Previous studies have reported that the presence of high ion concentrations, particularly Cl^- ions, in human blood can easily degrade most magnetic materials employed in magnetic biomedical MNSs.[112,113]

The effects of phosphate and calcium species on metallic biomaterials in body fluids are intriguing, particularly for metallic MNSs with unique shapes and small sizes, where they can hinder or protect the materials.[39] A transient and unstable protection strategy (because of human dynamic physiological conditions) using inorganic species can help in decreasing the high susceptibility of metallic MNSs to rapid dissolution in aggressive human biological media.[23] Previous studies have revealed that metal-phosphate and metal-calcium/phosphate films can form on metal oxide surfaces (such as TiO_2 and Cr_2O_3) due to the adsorption of phosphate ($H_2PO_4^-$ and HPO_4^{2-} at pH ~7) and calcium species. These films create a protective and complex layer that is thin and compact.[23,114] This protective layer acts as a barrier, inhibiting electrochemical reactions and blocking the mass transport of oxygen or reaction products within the passive film, thus significantly enhancing corrosion resistance.[23] Previous research on the corrosion stability of magnetic NiCo pillar-based microrobots indicated that upon immersion in a phosphate-buffered saline (PBS) solution, the surface of the microrobots remained relatively uniform, with a thick oxide-phosphate layer detected through EDXS analysis. However, the presence of small pits of reduced dimensions could be attributed to the attack of Cl^- ions.[22] These findings suggest that the formation of phosphate-oxide film complexes by phosphate species can effectively mitigate the severe corrosion and biodegradation mechanisms of small-scale swimmers in human biological media.

pH is another factor that influences the corrosion and biodegradation behaviors of metallic biomaterials, particularly metallic MNSs.[110] pH plays a critical role in the metal ion release from metallic biomaterials via different routes, including direct dissolution through protonation or indirect dissolution through the change in the surface charge (zeta potential) on both metallic surfaces and complex agents or proteins.[71,107,115] In general, the presence of released metal ions at high concentrations leads to a reduction in the pH value around tissues close to damaged biomaterials.[116] A previous study investigated the corrosion stability and functional properties of helix-shaped Cu nanoparticles (average size: ≈100 nm) after 20 min of immersion in two different solutions, including water and an acidic PBS solution (pH 3.5), via circular dichroism spectroscopy (sensitive probe of the structure and symmetry of nanocolloids).[44] Results demonstrated that the spectral peak of Cu nanoparticles in the PBS solution was strongly diminished compared with that in water, which indicates a higher dissolution of Cu nanoparticles. Another study showed a direct relationship between the performance (swimming speed) of tubular polyaniline/Zn microrockets and environmental pH (hydrochloric acid (HCl) solution and pH range −0.2 to 1.4), which was attributed to the higher Zn dissolution and, in turn, more H_2 bubble formation with an increase in the pH.[117]

Note that MNSs circulation in the body is closely related to their corrosion/biodegradation rate and the corrosivity of the environment they are exposed to (Tables 1 and 2). MNSs with a high degradation rate in a practical or simulated environment experience a decline in their velocity and circulation time, which ultimately leads to reduced targeting efficiency and performance (Tables 1 and 2). For example, research has reported on the corrosion/biodegradation, velocity, and circulation time of biodegradable Mg-based micromotors [32,92] and Fe-based magnetic

Table 2. The degradation mechanisms of MNSs and micro- and nanomaterials with different chemical compositions in various physiological environments.

Shape and size	Chemical composition	Physiological media		pH and T	Targeting ability	Aggregation time	Degradation time	Degradation mechanism by species	Ref.
		In/ex vivo	In vitro						
Nanoparticle	Citrate-coated iron oxide	-	Acidic citrate buffer	4.7 and 37 °C	Lowest magnetic response (MR) after 22 days	10 days (protein-induced aggregation)	30 days (average value of different apoferritin ratios)	Apoferritin and Holoferritin metal ions up-take or release	[151]
Nanoparticle	CFO	Livers and spleens	Acidic citrate buffer	4.7 and 37 °C	Lowest MR after 30 days	7 days	75 days (spinel structure changes after 75 days)	Apoferritin and Holoferritin metal ions up-take or release	[42]
Nanoparticle	Iron oxide	Livers and spleens	-	7.2 and 37 °C	Lowest MR after 7 days (liver) and 30 days (spleen)	-	30 days (liver) and 90 days (spleen)	Ferritin, cells and macrophages	[153]
Nanoparticle	Iron oxide	Astrocytes brain cell	-	7.2 and 37 °C	-	7 days	-	Ferritin and astrocytes cell	[193]
Nanoparticle	Iron oxide	Human Mesenchymal stem cells (Lonza)	Acidic citrate buffer	4 and 37 °C	Lowest MR after 15 days	10 days	22 days (Chondrogenesis process)	Ferritin and stem cell	[194]
Nanoparticle	Fe/Au	liver, spleen, kidney, andlung	Acidic citrate buffer	4.7–7.4 and 37 °C	Lowest MR after 30 days	1 day	30 days (Iron) and 180 days (Au degraded to small particles)	Ferritin (Iron), hepatic and splenic lysosomes (gold)	[142]
Nanoparticle	Cu and Ag	-	100 mM $NaClO_4$ + 1 mM HCl	Acidic solution and room temperature	-	-	360-420 s (at 0.3 V vs Ag/AgCl)	Uniform corrosion or electrochemically dissolution	[195]
Nanowire	Iron oxide	NIH/3T3 fibroblast cells	-	1.4–9.1 and 37 °C	-	1 day	1 day (They degraded to small particles)	Uniform corrosion, particularly fibroblasts and acidic pH effect	[152]
Janus microball	Pt/TiO_2	-	5 wt% H_2O_2	7 and 23 °C	Lowest velocity after 16 days (under UV irradiation)	-	-	Localized/Galvanic corrosion, H_2O_2 inflammatory impact	[30]
Microtubes	Cu/Pt and Pt/Fe/Cr/Pt	-	Distilled water (DS), DS+1.15%SDS and DS+ 1.15%SDS+ 7.76% H_2O_2	7 and room temperature	-	-	7 days (Cu/Pt -Cu 54.2% corroded, Pt/Fe/Cr/Pt-Cr 29.2% and Fe 78.6% corroded) in H_2O_2	Localized/Galvanic corrosion, H_2O_2 inflammatory impact	[17]

(*Continued*)

Table 2. (Continued).

Shape and size	Chemical composition	Physiological media		pH and T	Targeting ability	Aggregation time	Degradation time	Degradation mechanism by species	Ref.
		In/ex vivo	In vitro						
Nanorods/helice	Cu/Ti/HfO_2 and Co/Ti/HfO_2	-	PBS	3.7 and room temperature	Lowest MR (Co) and LSPR signal (Cu) after 6 h and 4 h	-	14 h (Co, un-protected) and 16 h (Cu, un-protected)	Localized/Galvanic corrosion,	[44]
Microtubes	Pt	-	5 wt% H_2O_2	7 and 25 °C	Lowest velocity after 25 days	-	-	Localized corrosion	[121]
Micropillars	NiCo and NiCo/Au	-	PBS+ 1 g L^{-1} BSA	7.4 and 37 °C	Lowest MR after 30 days	-	-	Localized/Galvanic corrosion, biodegradation process by protein	[22]

microrobots [58] in gastric acid medium, a highly corrosive environment with a pH of 1–3. Microscopy results revealed that helical Fe-based magnetic microrobots experienced intense corrosion, with the formation of dark brown iron corrosion products, after only 20 min of immersion in this medium (as shown in **Figure 4**A). Additionally, the velocity monitoring results of Mg-TiO_2 Janus micromotors in simulated gastric media (pH ~1.3) demonstrated an approximate lifetime of 6 min for this micromotor due to continuous hydrogen reaction (Mg corrosion process and supporting electron for hydrogen evolution reaction) and generation of microbubbles (as shown in Figure 4B). These findings suggest that the tendency of MNSs to corrode and biodegrade in different environments can significantly affect their circulation time, velocity, and ultimately, their performance.

3.3.2. ROS and Fenton reactions

The production of reactive oxygen species (ROS) such as superoxide anions (O_2^-), hydroxyl radicals (·OH), and hydrogen peroxide (H_2O_2, extracellular H_2O_2 is in the range of μM–mM) is triggered by the activation of inflammatory cells, including macrophages, neutrophils, and oral bacteria.[23,118] ·OH radicals are powerful oxidizing species that can oxidize most biological organic species such as proteins and DNA.[119] In particular, the use of H_2O_2 as a strong oxidant can significantly diminish the corrosion resistance behavior of metallic biomaterials, such as CoCrMo, Ti alloys, and stainless steel, owing to the formation of a rougher, thicker, and more porous surface oxide film.[78,120] Considering the small size of metallic MNSs, the presence of H_2O_2 agents as self-propelled fuel sources and/or ROS in human physiological media can remarkably accelerate the metal ion release and degradation of these tiny devices (Table 2).

A previous study on metallic MNSs showed that the velocity of Pt/TiO_2 Janus micromotors decreased when exposed to Milli-Q deionized water under different conditions and immersion times (1, 5, 10, and 15 d) due to the high degradation of the Ti region (Figure 4C).[30] However, the average velocity of the Pt/TiO_2 Janus micromotors remained relatively constant in a 5 wt% H_2O_2 environment. This was due to the fact that the propulsion mechanism depends only on the decomposition process of H_2O_2 on the Pt surface and is not affected by the surface physical and chemical evolution of Pt/TiO_2 Janus micromotors.[30] Another study investigated the corrosion stability behavior of self-propelled Pt/Cu and Pt/Ti/Cr/Fe microswimmers after 7 days of immersion in various environments, including distilled water, 1.15 wt% sodium dodecyl sulfate (SDS), and 7.76 wt% H_2O_2 +1.15 wt% SDS [17] (Figure 4D). The highest release of Pt, Cu, Ti, Cr, and Fe ions occurred from both microswimmers in 7.76 wt% H_2O_2 +1.15 wt% SDS, followed by 1.15 wt% SDS, and then distilled water. This can be attributed to the highly corrosive properties of the H_2O_2 agent. A previous investigation also examined the role of H_2O_2 in the corrosion stability and catalytic activity of Pt tubular microrobots in 3 and 5 wt% H_2O_2 environments [121] (Figure 4E). Results demonstrated that the velocity of Pt tubular microrobots decreased from 90 μm s^{-1} to 40.1 μm s^{-1} and 117.5 μm s^{-1} to 45.9 μm s^{-1} after 28 days of immersion in both 3 and 5 wt% H_2O_2 environments, respectively.

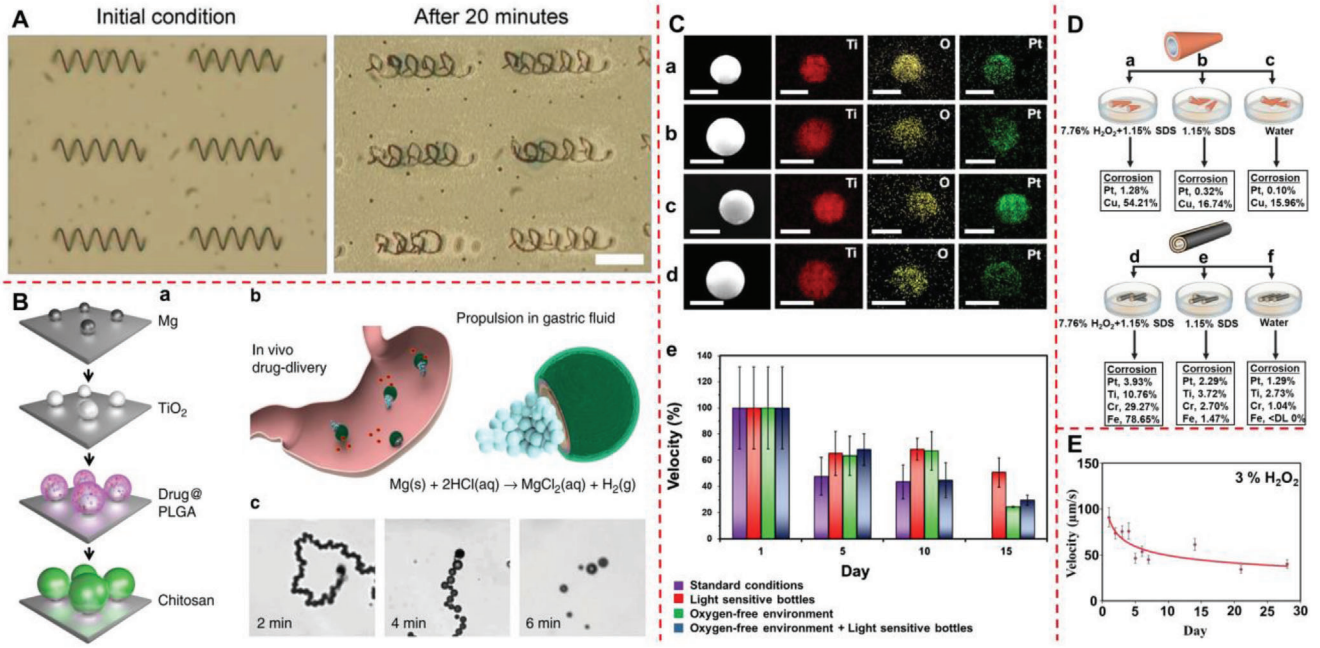

Figure 4. A) Fe helical microrobot degradation in simulated gastric liquid before and after 20 min. The scale bar corresponds to 50 µm. Adapted with permission.[58] Copyright 2019, Wiley-VCH GmbH. B), (a) Schematic representation of the preparation of micromotors: dispersion of Mg micromotors over a glass matrix, atomic layer deposition of TiO_2 over the Mg micromotors, drug-loaded PLGA deposition over the Mg-TiO_2 micromotors, and chitosan polymer deposition over the Mg-TiO_2-PLGA micromotors, (b) Schematic representation of in vivo propulsion and drug delivery of the Mg-based micromotors in a mouse stomach. (c) Time-lapse images of the propulsion of the drug-loaded Mg-based micromotors in simulated gastric fluid (pH ~1.3). Adapted with permission. [32] Copyright 2017, Springer Nature. C) SEM-EDXS images of (a) 1 day, (b) 5 days, (c) 10 days, and (d) 15 days Janus Pt/TiO_2 microrobots with corresponding elemental composition mappings of Ti, O, and Pt. Microrobots were stored in Milli-Q deionised water at room temperature. Scale bars represent 2.5 µm. (e) Average velocities of Pt/TiO_2 Janus microrobots in the different immersion times (days) under effect of UV irradiation in water or standard condition (violet), light sensitive bottles (red), in oxygen-free environment (green), oxygen-free environment + light sensitive bottles (blue). Adapted with permission.[30] Copyright 2020, Elsevier. D) Corrosion of self-propelled Pt/Cu (a–c) and Pt/Ti/Cr/Fe (d–f) microjets in various environments, including pure water, 1.15% SDS and 1.15% SDS + 7.76% H_2O_2. Adapted with permission.[17] Copyright 2013, The Royal Society of Chemistry. E) Velocity evaluation of Pt tubular micromotor during exposure to 0.25% SDS + 3% H_2O_2 media over a period of 28 days. Adapted with permission.[121] Copyright 2018, The Royal Society of Chemistry.

Iron plays a key role in producing advanced biomaterials for diverse fields, including biocatalysis,[122] biosensing,[123] surgical implants,[124] micro and nanoparticles/swimmers with various medical applications, such as magnetic resonance imaging (MRI) contrast agents,[125] and drug delivery systems.[126] However, the release of iron ions in the biological media resulting from the interactions with special proteins, i.e., ferritin or metallic biomaterials, can exacerbate the inflammatory condition due to ROS generated from the Fenton reaction.[41] This reaction refers to the reaction between the iron ions (Fe^{2+}) and H_2O_2 to produce highly oxidizing agents such as $\cdot O_2^-$ and ·OH, as follows:[127,128]

$$Fe^{2+} + H_2O_2 \rightarrow Fe^{3+} + \cdot OH + OH^- \quad (1)$$

The synergistic effect of the Fenton reaction and cell-released chemical species can induce inflammatory-cell processes, resulting in a significant adverse impact on the corrosion stability of metallic biomaterials, particularly iron and iron oxide nanoparticles[41,126] (Table 2). A previous study investigated the influence of surface functionalization on the chemical stability of iron oxide nanoparticles in various media. Results revealed that the nature of surface functionalization (e.g., citrate, ascorbate) can severely enhance ROS production during Fenton reactions.[129] In contrast, glucose-coated iron oxide nanoparticles exhibit negligible ROS generation through the Fenton reaction compared to uncoated iron oxide nanoparticles.[130] The high level of ROS generation in human physiological media also causes oxidative damage to cellular constituents and disrupts cell metabolism, but it can also potentially kill cancer cells.[131] Fe_3O_4 nanoparticles have been widely employed for the generation of toxic ROS in cancer therapy.[24,132] The iron ions released from iron and iron oxide nanoparticles during interactions with H_2O_2 lead to the generation of ·OH via the Fenton reaction, which acts as an inhibitor of cancer cells.[31,133]

3.3.3. Protein Nano-Biofilm and Macrophage/Cell Substances

When surgical implants ranging from large-scale to micro- and nano-sized biomaterials are transplanted into human physiological media, the first event is the adsorption of protein molecules onto the surface of the biomaterial. These protein molecules directly determine the following events on the biomaterial surface.[134] The subsequent cell-surface interaction and lifespan of biomaterials can be significantly influenced by the formation of protein adsorption and protein nano-biofilm.[135]

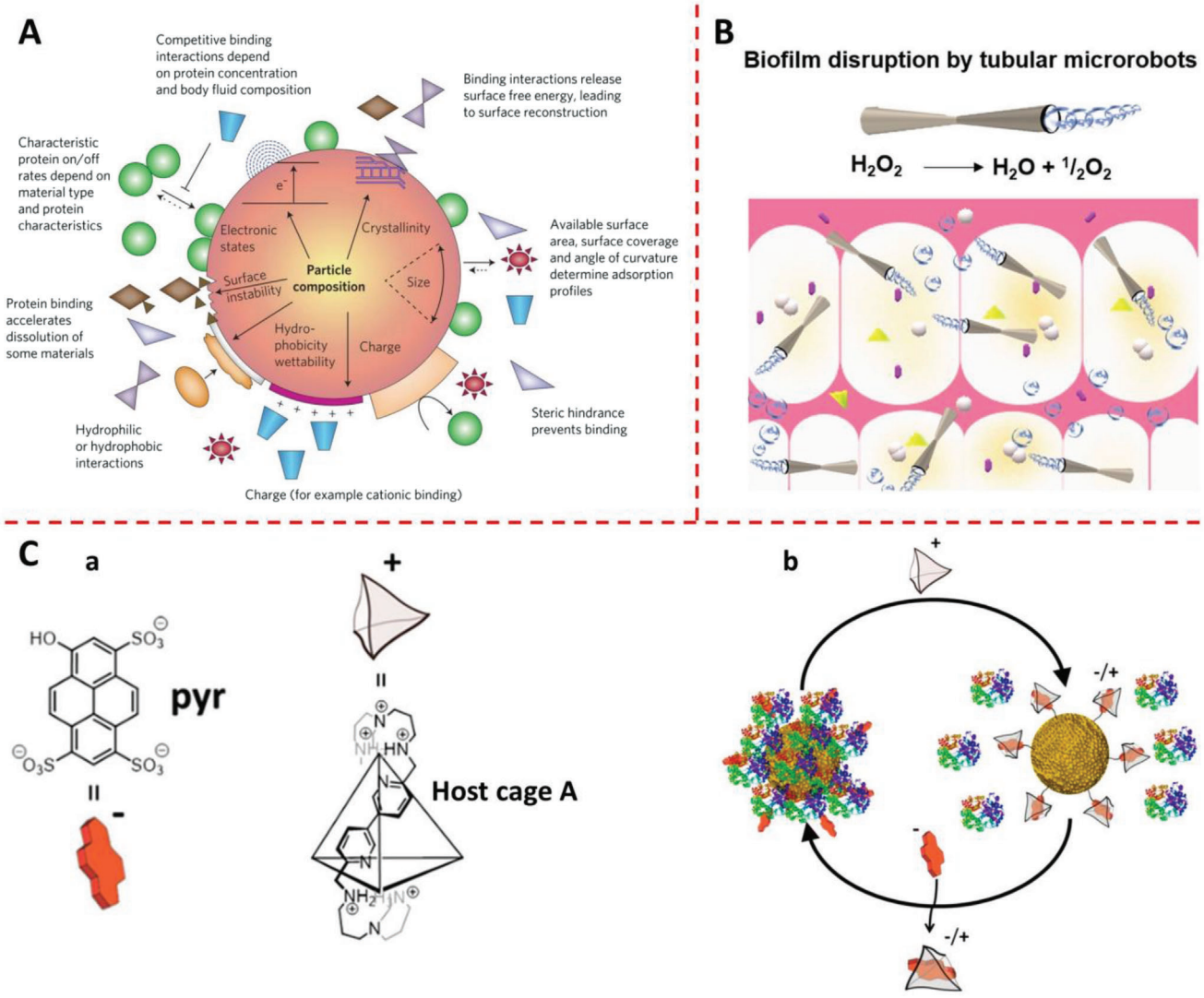

Figure 5. A) Material characteristics of MNSs that influence the chemical stability and functional properties of these tiny machines. These initial characteristics contribute to the formation of protein corona in a human complex physiological media. Adapted with permission.[95] Copyright 2009, Springer Nature. B) Self-propelled tubular Pt-TiO_2 microrobots. The killing/removing ability of these micromachines is ascribed to their antibacterial activity and the continuous generation of microbubbles at the biofilm surface. Adapted with permission.[140] Copyright 2020, Elsevier. C) (a) Chemical structures of the guest molecule pyr and the host cage A (the chemical structure of only one edge of the tetrahedral cage A is shown for clarity). b) Schematic representation of the reversible control over protein corona formation on Au nanoparticles, using a supramolecular host-guest complex between negatively charged pyr and positively charged cage A. Adapted with permission.[141] Copyright 2020, American Chemical Society.

The instantaneous adsorption of proteins from human biological environments on biomaterial surfaces remarkably influences the biocompatibility of biomaterials.[136,137] Protein nanofilms adsorbed on biomaterial surfaces significantly enhance osteoblast cell attachment, proliferation, differentiation, and bone tissue regeneration.[135] Moreover, the adsorbed protein layer plays a critical role in the physiological roles of implanted/injected biomaterials in biological media, including coagulation, thrombogenesis, and inflammatory responses.[138] Additionally, protein denaturation, fragmentation, and conformational arrangement during adsorption onto biomaterial surfaces may influence the function of the host body.[139] The characteristics of metallic small-scale swimmers can significantly influence protein interactions (**Figure 5**A).[95] MNSs can be customized by adjusting their chemical composition, surface functionalization, and motion mechanism. This enables them to degrade both thin and thick biofilms on their surfaces, as well as remove biofilms in the environment (Figure 5B,C). For example, Villa et al. developed TiO_2/Pt self-propelled micromotors that effectively eliminate dental biofilms by generating hydroxyl radicals and microbubbles on the biofilm surface.[140] These microbubbles and H_2O_2 act as repulsive agents, which prevent protein nano-biofilm formation on the micromotor's surface. In a similar vein, Jesus et al. prevented the formation of protein corona (protein nano-biofilm) on Au nanoparticles by using a supramolecular host-guest complex that interacts with positively

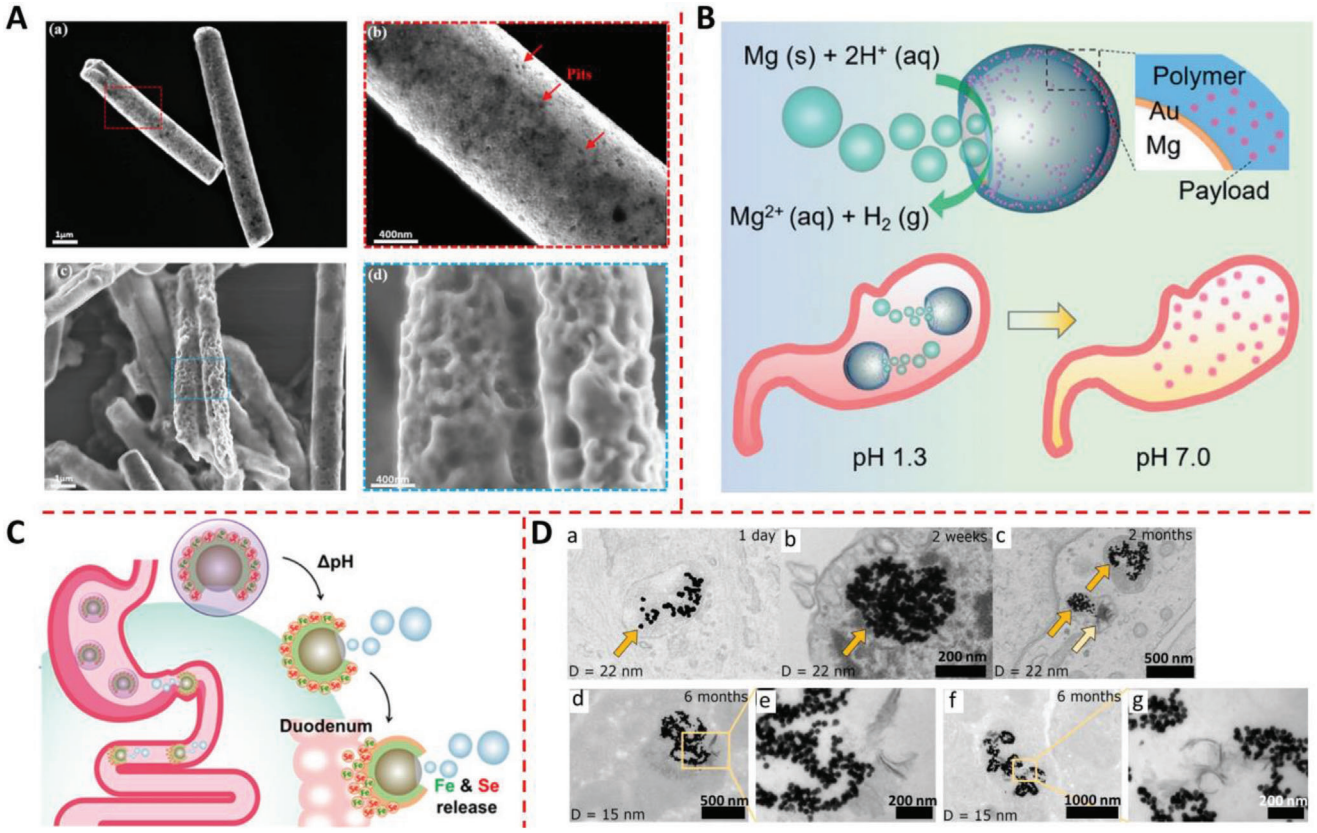

Figure 6. A) Low and high magnification field emission (FE-SEM) images of NiCo-MPs after immersion in (a,b) PBS and (c,d) PBS + BSA solution for 56 days. Adapted with permission.[22] Copyright 2021, Elsevier. B) Representations of an acid-powered Mg-based Janus micromotor and its acid neutralization mechanism. This Janus micromotor is produced by an Mg microsphere coated with a thin Au layer and a payload-encapsulated pH-sensitive polymer layer. Adapted with permission.[92] Copyright 2017, Wiley-VCH GmbH. C) Schematic illustration of micromotor-based in vivo delivery and release of Fe and Se at the duodenum region. The micromotor consists of a Mg/TiO_2 core protected with an inner PLGA polymer layer, a middle chitosan layer loaded with Fe and Se, and an outer pH-responsive enteric layer. Adapted with permission.[144] Copyright 2019, American Chemical Society. D) TEM images of human fibroblasts exposed to gold nanoparticles with sizes of 22 or 15 nm disclose the presence of diffuse areas correlated to the degradation process (a–c). TEM observations of representative lysosomes/gold nanoparticles (22 nm) detected in (a) 1 day, (b) 2 weeks, and (c) 2 months, indicating the two different regions including dense areas (dark orange arrows) and diffuse areas (light orange arrow). Some diffuse areas were detected after 2 months of exposure time with 22 nm gold nanoparticles. (d–g) TEM images of lysosomes observed 6 months after 15 nm gold nanoparticles exposure, indicating dense and diffuse areas at two different magnifications. Adapted with permission.[43] Copyright 2020, National Academy of Sciences.

charged supramolecular cages and surface-exposed pyranines (Figure 5C).[141]

Protein adsorption on solid surfaces is a complex process involving electrostatic, hydrophobic, van der Waals, and hydrogen bonding interactions.[23] In high protein concentration environments like human blood, MNS motion may be affected by the formation of denser and thicker protein nano-biofilms, as opposed to lower protein concentration environments such as ocular or bronchial fluids.[95] However, the adsorption/interaction of protein molecules on metallic biomaterial surfaces can significantly affect their corrosion performance.[23,120] Protein molecules can enhance the degradation and metal ion release of metallic biomaterials by participating in electrochemical dissolution and/or chemically enhanced dissolution processes.[135] Our previous study on the corrosion performance of magnetic NiCo micropillars in BSA media (1 g L^{-1}) revealed that the BSA protein accelerated the biodegradation and Ni/Co ion release process due to protein-metal bonding and detachment of protein-metal complexes, eventually leading to a severely grooved surface (**Figure 6**A).[22] Protein adsorption and nanofilm formation on the surface of large- and small-scale biomaterials can significantly diminish their corrosion resistance behavior by hindering the protective effect of phosphate species (complex phosphate thin films), thereby resulting in accelerated degradation processes.[22,23]

The corrosion and biodegradation processes of MNSs are significantly affected by their interaction with large biological species, such as cells and macrophages, as well as the highly acidic and complex environments that contain proteins, enzymes, and other compounds (Table 2). MNSs may undergo a special structural and morphological transformation in in vivo media, such as dissolution (metal ion release), degradation, dissociation, and agglomeration.[142] Several studies have reported the degradation, toxicity, biodistribution, and biotransformation of metallic and oxide MNSs and nanoparticles in in vitro and in vivo media such as complex self-assembled–magnetite–

gold Janus microcapsule,[143] Mg/TiO_2-PLGA-enteric coating,[144] Mg/Au-enteric layer,[92] gold,[43] silica,[145] iron oxide,[146] anatase, and rutile titanium dioxide nanoparticles.[147] Previous investigations on acid-powered micromotors (mainly Mg-based) in gastrointestinal fluids represented that the corrosion rate (direct correlation with Mg dissolution) and velocity (dissolution of Mg and then bubbles formation) of these self-propelled micromotors are affected by the pH of stomach media that strongly influence their temporary targeted-delivery performance (Figure 6B,C).[92,144] Likewise, a previous study investigated the degradation of gold nanoparticles with sizes between 4 and 22 nm in vitro by human cell lysosomes to verify whether gold nanoparticles with superior chemical inertness, particularly in an aggressive environment, are susceptible to degradation and bio-dissolution.[43] TEM results demonstrated the intracellular degradation of gold nanoparticles during 2–6 months of incubation in primary human fibroblasts due to ROS generation by a membrane protein assembly termed NADPH oxidase, which oxidizes gold nanoparticles into released gold ions (Au^+ or Au^{3+})[43] (Figure 6D).

In the case of nanoparticles, particularly magnetic nanoparticles, one major obstacle is the gradual reduction in the corrosion stability and loss of targeting potential in complex human biological media.[148–150] According to previous reports,[42,151,152] most magnetic nanoparticles were detected within the spleen and liver, where they settled intracellularly within the endosomes. After a certain incubation time, acid-induced degradation gradually occurs during the interaction of nanoparticles with lysosomes[148] (Table 2). Following in vivo degradation, iron oxide nanoparticles progressively lose their magnetic properties at the targeted site of the body because of their degradation in the acidic lysosome environment, particularly in splenic and hepatic macrophages.[42,153] The ferritin and/or apoferritin protein (ferritin protein empty of iron ions) in the intracellular degradation mechanism of iron oxide nanoparticles (in the liver and spleen) significantly influences the long-term durability and functional properties (e.g., magnetic properties) of these nanoparticles.[142] A previous study investigated the degradation events of magnetic $CoFe_2O_4$ ceramic nanoparticles upon apoferritin protein storage of both Fe and Co under in vitro conditions in an acidic citrate medium for 5 days at pH 4.7 and 37 °C[42] (**Figure 7**A). High-resolution scanning transmission electron microscopy (STEM)/EDXS analysis results at the nanoscale demonstrated the degradation process of $CoFe_2O_4$ nanoparticles due to their dissolution in an acidic citrate medium and the metal ion transfer mechanism at the nanoparticle solid/apoferritin interface (metal ion uptake process). Another study demonstrated the long-term chemical stability of gold (core)/iron (shell) oxide heterostructures after intravenous injection in mice [142] (Figure 7B). Based on the achievements related to Au/Fe nanoparticle degradation in the liver and spleen, a two-stage biodegradation process was disclosed, including the primary dissolution of the iron oxide layer around the gold core and the secondary degradation of 5 nm gold particles in the form of small particles. In addition, some studies demonstrated the effect of cell substances in in vitro medium on the mechanical response of helical micro (SiO_2/Fe)[154] and nanorobots (FePt)[155] in a magnetic field after a certain time of implantation in this intracellular environment (Figure 7C,D). In both case studies, the results showed that the micro and nanorobots partially or completely lost the magnetic response due to two separate or simultaneous occurrences including i) the dissolution of the magnetic part (e.g., iron) by leaching and ii) cell adhering action. Regarding the cell adhering action, they identified cells that had internalized helical SiO_2/Fe microrobots that did not respond to magnetic fields. After adding 0.1% SDS solution as a treatment process, they observed an instantaneous lysing of the cell, which allowed the helical SiO_2/Fe microrobots to respond to the magnetic field again.

4. Stability Optimization

4.1. Surface Protection

As previously explained, combinations of critical factors can strongly affect the corrosion resistance behavior of these small-scale swimmers, limiting their application. Furthermore, due to their small sizes, their functionalities are particularly compromised by their corrosion and biodegradation and thus, their stability in various environments needs to be improved. Accordingly, different strategies can be developed to achieve ideal MNSs with high corrosion and biodegradation resistance. These strategies include the use of materials that are thermodynamically hard to corrode (e.g., more noble metals such as Au, Pt, Ir, Rh, and Ag) and protection via the application of a barrier thin film of organic and inorganic (e.g., oxides) materials. However, compared to using noble metals, the barrier film approach has numerous benefits, including the ability to freely select medium electrochemically active and passive materials, lower use of expensive materials as they are applied as films, cheap and effective materials for propulsion, and various functional properties for targeted applications. The barrier film strategy is conventionally divided into three approaches based on the nature of the protective films: metallic, oxide-coated, and organic thin films, as will be discussed below.

4.1.1. Metallic Thin Film Coatings

The application of metallic thin film coatings on the matrix of micro- and nanomaterials has been widely explored for a wealth of different potential functionalities in biosensors, catalysis, energy storage, and MNSs in environmental and medical applications.[156–159] In the case of core-shell nanoparticles, multiple functionalities can be established owing to the synergistic effect of both the core and shell components, enabling them to have versatile applications.[160] In an earlier research, noble shell metals such as Au, Pt, Pd, and Ag were utilized to encase Fe and Cu core nanocrystals, with a thickness of ≈5–10 nm, for various technological applications. These metals demonstrate exceptional resistance to corrosion and biodegradation, particularly in human physiological media, highlighting their high corrosion stability.[158] In addition, as reported in previous research, utilizing the Co magnetic core and noble metals as shells into Co@Au, Co@Pd, Co@Pt, and Co@Cu nanoparticles not only reveals the various potential functionalities such as magnetic storage, MRI, and cell separation vectors in these nanoparticles, but can also help in achieving specific properties in terms of catalytic and long-term corrosion and biodegradation stability.[160] Metallic thin films coated on active materials were also investigated

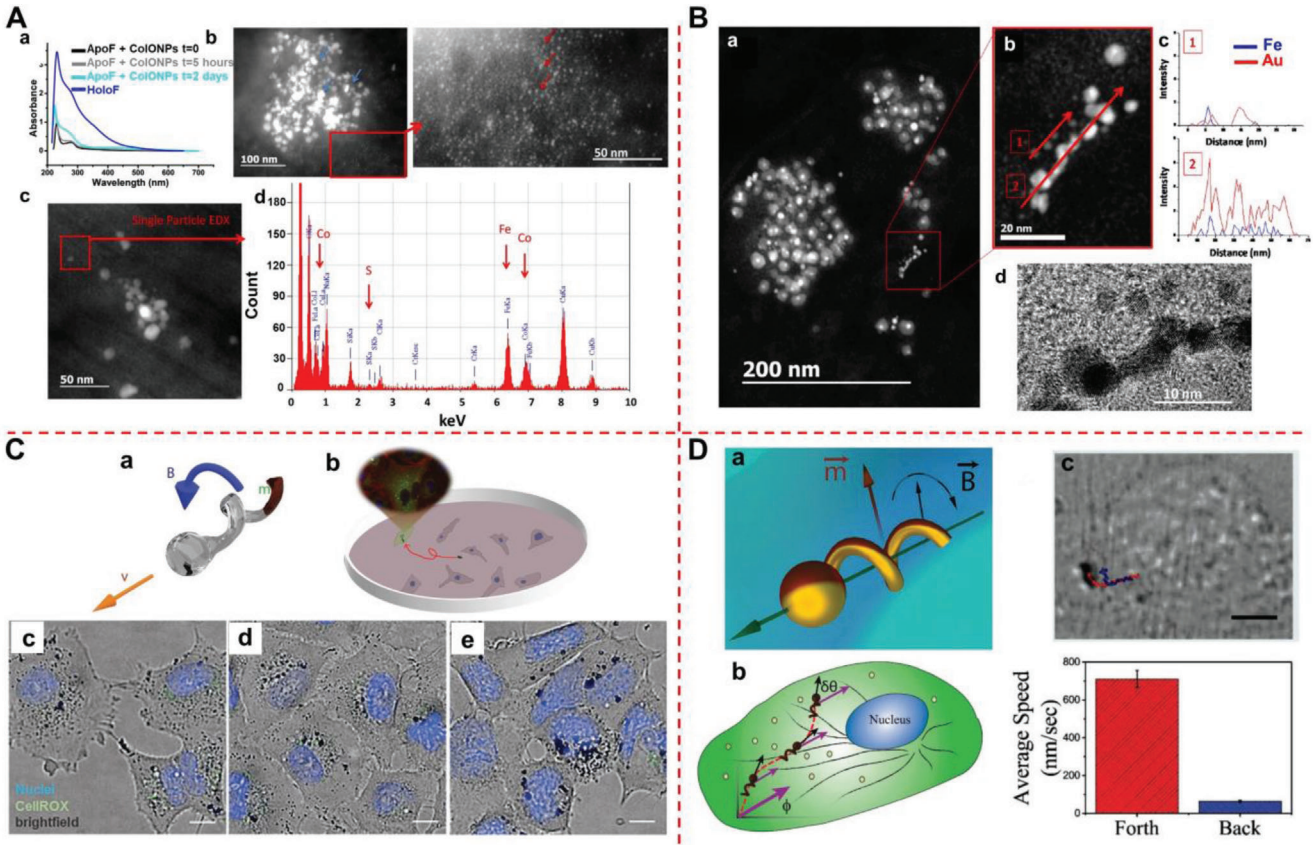

Figure 7. A) Transfer of metal ion from CFO nanoparticles to apoferritin protein. a) UV–Vis spectra of apoferritin incubated with CFO nanoparticles in acidic medium for 5 h and 2 days. Compared to apoferritin and Holo-ferritin, the growth of absorbance shoulder at 280 nm presents a metal filling process by the apoferritin protein. b) STEM-High-angle annular dark-field (HAADF) images of CFO nanoparticles (blue arrows) incubated with apoferritin for 2 months, red arrows indicate the metal-filled proteins as small particles. c,d) STEM and EDXS analysis of single particle presented in the red-contoured area to confirms the occupancy of Fe, Co, and S in single apoferritin with of 64.7%, 28.2%, and 7.13% (at%), respectively. Adapted with permission.[42] Copyright 2017, Springer Nature. B) Two-stage element-specific biodegradation of nanoheterostructures (NHs): first stage, dissolution of iron oxide around gold core detected after 14 days exposure in spleen media. a) STEM-HAADF image of a splenic lysosome reveals intact NHs close to chain-forming bright residues (red square). b) High magnification image from the red square in (a). c) STEM-EDXS analysis on line 1 and 2 in (b). d) High-resolution TEM image which confirms the presence of some gold particles that still have interfaces with iron oxide, while others consist of pure gold monocrystals. Adapted with permission.[142] Copyright 2015, American Chemical Society. C) (a) Representation of FePt nanopropellers that display high magnetic moments *m* that enable movement via small external rotating magnetic fields *B* and (b) navigation of FePt nanopropellers through cell media, transfect cells, and deliver genetic material. c–e) Cells incubated with uncoated particles at a 50:1 ratio for (c) 24 h, (d) 48 h, or (e) 72 h. Scale bar corresponds to 10 µm. Adapted with permission.[155] Copyright 2020, Wiley-VCH GmbH. D) (a) Schematic illustration of nanomotor actuation driven by small rotating magnetic fields (SiO_2 is shown in yellow and a thin film of iron with magnetic behavior deposited on the SiO_2 is shown in brown). b) Schematic representation of the difference between intended direction and achieved direction $\delta\theta$ as the motor moves inside a cell. Violet and blacks arrows indicate intended and achieved directions, respectively. c) Significant decrease in pitch as the nanomotor trajectory is reversed inside a HeLa. Scale bar corresponds to 5 µm. Adapted with permission.[154] Copyright 2018, Wiley-VCH GmbH.

by applying an Ag-coated shell on Fe core nanoparticles for applications in optoelectronics, spintronics, and biomedicine.[161] The multifunctional properties of Fe@Ag core-shell nanoparticles were demonstrated through their enhanced plasmonic sensitivity and tunability, as well as their adjustable magnetism.[159] These nanoparticles displayed exceptional stability and maintained their functional properties over extended periods when used in complex human body fluids for various applications such as MRI, drug delivery, protein separation, and magnetic hyperthermia. Moreover, their higher resistance to corrosion and biodegradation makes them a promising candidate for biomedical applications. In another study, it was found that depositing a Pt shell on Fe core nanoparticles can lead to the creation of novel properties while maintaining a low-cost production process, high catalytic activity, long-term corrosion stability, and ease of recovery. Furthermore, our previous investigation on the corrosion and biodegradation behavior of magnetic swimmers showed that the presence of a thin layer of coated Au (≈100 nm) on NiCo micropillars in albumin protein media resulted in a significant reduction of corrosion and biodegradation rates, metal ion release, and protein-related detrimental effects when compared to non-coated NiCo micropillars. Remarkably, this effect was observed even in the presence of micro and nano defects and over long-term exposure to protein media[22] (**Figure 8**A).

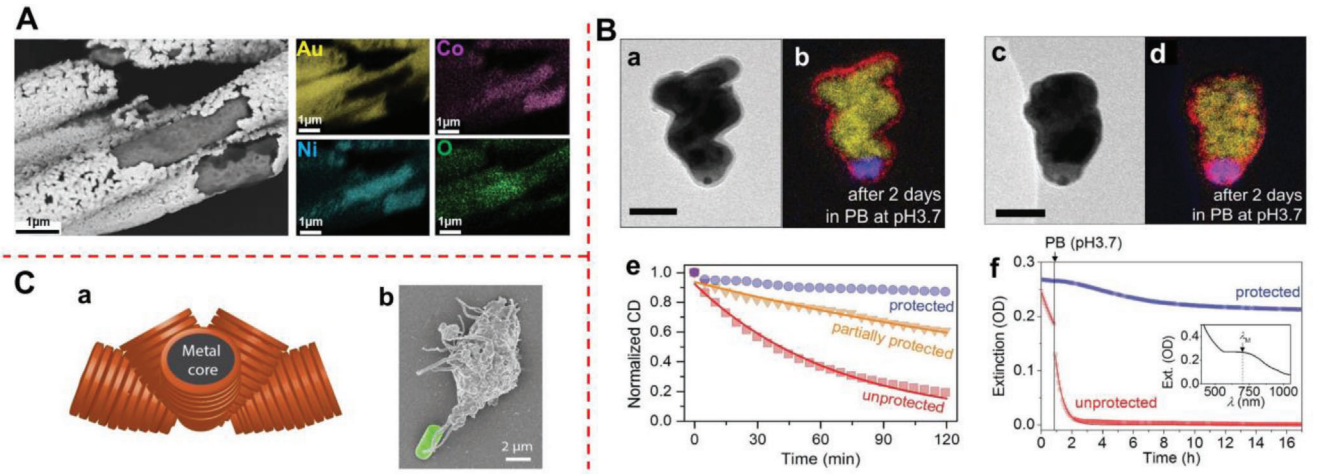

Figure 8. A) SEM micrograph and EDXS elemental maps of NiCo/Au-MPs after immersion in PBS+BSA solution for 56 days. Adapted with permission.[22] Copyright 2021, Elsevier. B) TEM images of (a,b) protected helix-shaped Cu nanoparticle by HfO_2 and (c,d) protected Cu nanorod by HfO_2. EDXS elemental map (yellow: Cu, blue: Ti, red: O, scale bar: 50 nm). e) Normalized circular dichroism spectra of helix-shaped Cu nanoparticles. f) Optical extinction spectroscopy of Cu nanorods. Adapted with permission.[44] Copyright 2017, Wiley-VCH GmbH. C) (a) Schematic side view of rod-shaped NiCo-SiO_2 magnetic microrobot. b) SEM image of a macrophage-prey encounter. Adapted with permission.[169] Copyright 2017, American Association for the Advancement of Science.

4.1.2. Oxide Thin Film Coatings

One method for protecting MNSs against corrosion and biodegradation involves applying a thin film of inert oxide materials such as HfO_2, Al_2O_3, TiO_2, and SiO_2.[157] Various techniques exist for producing high-quality oxide thin films, including chemical vapor deposition (CVD) and physical vapor deposition (PVD). However, atomic layer deposition (ALD) stands out as a powerful and well-controlled technique for corrosion and biodegradation protection of numerous biomaterials,[44,162] owing to its compatibility with a wide range of materials. This technique has gained considerable research attention in nanoscience and nanoengineering with wide application in nanosensors and electric conductors,[163] batteries,[164] catalysts,[165] and MNSs in medicine.[44] ALD has extensive applications in biomedicine and biotechnology, including biosensors and diagnostics (electrical detection of biologically relevant molecules). Additionally, ALD can facilitate the fabrication of nanoporous materials via surface engineering, biotemplating, and biomedical implants, such as orthopedic, dental, cardiovascular, and cochlear implants.[166]

In a previous study, HfO_2 and Al_2O_3 thin films were deposited by ALD to protect and improve the corrosion stability of Cu and Co nanorods and nanohelixes in a PBS solution [44] (Figure 8B). The results demonstrated that both HfO_2/Cu and HfO_2/Co nanorods immersed in PBS and acidic media for a week to over a month were stable, without loss of magnetic or plasmonic functionality. Another study employed an alumina ALD thin film (8 nm) to improve the oxidation resistance of iron nanoparticles.[167] The superior oxidation resistance of Fe/Al_2O_3 was also enhanced using this approach. Furthermore, high corrosion stability and particular functional properties can be anticipated for the application of these nanoparticles in biomedical diagnosis. Moreover, in another study, ZrO_2 nanoparticles were endowed with tunable chemical, electrical, and optical properties by coating the ZrO_2 nanoparticles with a continuous and homogeneous Al_2O_3 ALD thin film in the range of 5.8–18 nm (based on the typical AB cycles).[168] In another investigation, Schuerle et al. employed a plasma-enhanced chemical vapor deposition method for creating a thin layer of SiO_2 oxide on NiCo magnetic microrods which were finally coated by immunoglobulin G (IgG) molecules (Figure 8C).[169] The aim of using the SiO_2 oxide film on NiCo microrods (50 nm) was to reduce the Co and Ni ions release in mouse macrophage-like cells and preserve their high magnetic response efficiency (Corrosion process and formation of Ni and Co oxides strongly influence the motion of NiCo-SiO_2 microrods).

4.1.3. Organic Thin Films

Several studies have investigated the formation of organic thin films for surface functionalization on MNSs in biomedical applications. These films can improve the functional properties, selectively target biological entities, enhance chemical stability, biocompatibility, and reduce toxicity.[157,169,170] In a previous study, a magnetic NiCo micropillar pre-coated with anti-Escherichia coli IgG and covalently coupled with the tosyl group was employed to target macrophages and hinder the release of Ni and Co ions as toxic elements (corrosion stability).[169] Surface functionalization methods on smart nanoparticle materials, particularly metallic and oxide magnetic nanoparticles, have been widely studied for biomedical applications such as cell labeling, triggered drug delivery, and multimodal imaging.[156] According to a previous study, the covalent functionalization of materials such as chlorobenzene, nitrobenzene, and amino groups, on the surface of magnetic carbon-coated/Co (C/Co) nanoparticles resulted in enhanced magnetic properties and oxidation temperature behavior.[171] Nevertheless, C/Co nanoparticles as magnetic biomedical nanodevices have high corrosion resistance because of the noble behavior of the graphite layer (shell).

Note that when nanodevices are used in human physiological media, they immediately interact with proteins that form protein mono- or multilayers, termed as protein corona.[172] This protein corona can remarkably influence the size, aggregation state, functional or interfacial properties, and long-term stability of nanodevices in biological fluids.[173] A previous study reported the impact of surface chemistry and protein corona on the long-term biodegradation of iron oxide nanoparticles under both in vitro and in vivo conditions.[174] The results showed that glucose surface functionalization resulted in a lower degradation rate of iron oxide nanoparticles over four months in comparison to poly(ethylene glycol) functionalization, and the protein corona strongly influenced the biodegradation process of these nanoparticles. Other studies utilizing hydrophilic poly(ethylene glycol) surface functionalization on iron oxide nanoparticles achieved new improvements such as strong magnetic relaxivity, negligible nonspecific uptake by macrophages, biocompatibility, and superior long-term chemical stability in various biological media.[175]

4.2. Accelerating Deterioration

Ideally, it is desirable for MNSs to remain stable for a sufficient period of time to accomplish their desired tasks, and then rapidly degrade once their task is completed. The prolonged presence of nanomaterials within biological systems raises concerns about potential adverse effects on cell viability. Thus, the acceleration of nanomaterial degradation inside biological systems can mitigate potential adverse effects in tissues and organs (e.g., cell toxicity, and changes in cell phenotype and cell mobility).[176–178] To address this goal, Mattix et al.[179] reported surface modifications to accelerate the degradation of iron oxide nanoparticle through polymer encapsulation. They employed biodegradable coatings composed of Food and Drug Administration (FDA) approved polymers with different degradation rates: poly(lactide) or copolymer poly(lactide-co-glycolide). The generation of polymer degradation byproducts (lactic and glycolic acid) results in an acidic microenvironment within the polymeric nanoparticles. This acidic microenvironment facilitated the accelerated dissolution of iron oxide. The obtained results demonstrated that the degradation of iron oxide can be controlled by adjusting the content and composition of the polymers used for nanoparticle encapsulation. Then, the accelerated degradation observed in the coated iron oxide makes them a promising and biodegradable alternative for removing nanomaterials from tissues once their intended role is fulfilled.

Another possible strategy to enhance the degradation rate of metals is through alloying and composite formation.[180] For example, there are two primary approaches to reducing the corrosion resistance of iron[181]: 1) adding elements with lower electrochemical potential than Fe (−0.44 V vs SHE) that are soluble in iron to decrease the corrosion resistance of the matrix; 2) incorporating elements nobler than iron to create a second phase with higher electrochemical potential, leading to galvanic corrosion where iron is the anode and the nobler metal is the cathode. On this basis, Hermawan et al.[182] introduced Mn, which possesses an electrochemical potential lower than Fe, to develop a series of Fe–Mn alloys with the objective of achieving mechanical properties similar to those of stainless steel 316L but a degradation rate more favorable than that of pure Fe. The alloys, with Mn content between 20 and 35 wt%, exhibited higher corrosion current and lower electrochemical potential compared to pure Fe.

5. Summary and Outlook

Biomedical micro- and nanoswimmers (MNSs) have enormous potential for a wide range of applications, including targeted drug delivery, nanosurgery, localized biopsy, cell storing, and isolation of biological targets. However, to realize their full potential, MNSs must be biocompatible and capable of maintaining their functionalities throughout their lifetime within the complex physiological environment of the human body. Corrosion and biodegradation phenomena play a crucial role in determining the stability and functional properties of these tiny and smart devices.

Several factors affect the corrosion and biodegradation stability of MNSs in the human body, including their material and design characteristics, physical surface properties, and complex physiological media. Small-scale swimmer designs consist of combinations of critical aspects that can strongly affect their corrosion and biodegradation resistance behavior, limiting their application. To address this problem, various strategies can be employed to enhance and/or optimize the resistance of these MNSs to degradation, for example, including the use of materials that are thermodynamically hard to corrode and the application of a protective barrier thin film made of organic and/or inorganic materials on the entire surface of MNSs.

Understanding the degradation mechanism of MNSs and the factors affecting their degradation is essential for developing MNSs with appropriate degradation rates that are compatible with their intended applications within the human body, predicting their lifespan and performance, and preventing potential safety hazards that may arise if they degrade in the human body. However, to date, only a few studies have looked into the corrosion and biodegradation phenomena in motile micro- and nanostructures. Therefore, further research is required to explore additional strategies for achieving optimal MNS corrosion and biodegradation stabilities.

In conclusion, MNSs hold significant promise for various biomedical applications, but their corrosion and biodegradation behavior must be carefully investigated to ensure their optimal performance and safety within the human body. Further research in this area will help to develop better MNSs that can deliver improved biomedical outcomes.

Acknowledgements

This work was financially supported by the University of Udine, Italy and the ERC Consolidator Grant HINBOTs (No. 771565) and the MSCA-ITN training program "mCBEEs" (grant No. 764977). R.S.-G. thanks the Spanish Ministry of Universities and the European Union for a "Margarita Salas" postdoctoral fellowship (Next Generation EU).

Open access funding provided by Eidgenossische Technische Hochschule Zurich.

Conflict of Interest

The authors declare no conflict of interest.

Keywords

biodegradation, biomedicine, corrosion, small-scale swimmers

Received: September 5, 2022
Revised: June 26, 2023
Published online: July 12, 2023

[1] J. G. S. Moo, C. C. Mayorga-Martinez, H. Wang, B. Khezri, W. Z. Teo, M. Pumera, *Adv. Funct. Mater.* **2017**, *27*, 1604759.
[2] D. Xu, Y. Wang, C. Liang, Y. You, S. Sanchez, X. Ma, *Small* **2019**, *16*, 1902464.
[3] J. Katuri, X. Ma, M. M. Stanton, S. Sánchez, *Acc. Chem. Res.* **2017**, *50*, 2.
[4] S. Pané, J. Puigmartí-Luis, C. Bergeles, X. Z. Chen, E. Pellicer, J. Sort, V. Počepcová, A. Ferreira, B. J. Nelson, *Adv. Mater. Technol.* **2019**, *4*, 1800575.
[5] V. Agrahari, V. Agrahari, M.-L. Chou, C. H. Chew, J. Noll, T. Burnouf, *Biomaterials* **2020**, 120163.
[6] S. Wang, X. Liu, Y. Wang, D. Xu, C. Liang, J. Guo, X. Ma, *Nanoscale* **2019**, *11*, 14099.
[7] R. Sanchis-Gual, H. Ye, T. Ueno, F. C. Landers, L. Hertle, S. Deng, A. Veciana, Y. Xia, C. Franco, H. Choi, J. Puigmartí-Luis, B. J. Nelson, X.-Z. Chen, S. Pané, *Adv. Funct. Mater.* **2023**, 2212952.
[8] X. Wang, X. H. Qin, C. Hu, A. Terzopoulou, X. Z. Chen, T. Y. Huang, K. Maniura-Weber, S. Pané, B. J. Nelson, *Adv. Funct. Mater.* **2018**, *28*, 1804107.
[9] A. Terzopoulou, X. Wang, X. Z. Chen, M. Palacios-Corella, C. Pujante, J. Herrero-Martín, X. H. Qin, J. Sort, A. J. deMello, B. J. Nelson, *Adv. Healthcare Mater.* **2020**, *9*, 2001031.
[10] S. Gervasoni, A. Terzopoulou, C. Franco, A. Veciana, N. Pedrini, J. T. Burri, C. de Marco, E. C. Siringil, X. Z. Chen, B. J. Nelson, *Adv. Mater.* **2020**, *32*, 2005652.
[11] H. Wang, M. Pumera, *Chem. Rev.* **2015**, *115*, 8704.
[12] J. Li, B. E.-F. de Ávila, W. Gao, L. Zhang, J. Wang, *Sci. Rob.* **2017**, *2*.
[13] J. Li, I. Rozen, J. Wang, *ACS Nano* **2016**, *10*, 5619.
[14] J. Yong, A. S. Mellick, J. Whitelock, J. Wang, K. Liang, *Adv. Mater.* **2023**, *35*, 2205746.
[15] M. You, C. Chen, L. Xu, F. Mou, J. Guan, *Acc. Chem. Res.* **2018**, *51*, 3006.
[16] X. Z. Chen, B. Jang, D. Ahmed, C. Hu, C. De Marco, M. Hoop, F. Mushtaq, B. J. Nelson, S. Pané, *Adv. Mater.* **2018**, *30*, 1705061.
[17] G. Zhao, B. Khezri, S. Sanchez, O. G. Schmidt, R. D. Webster, M. Pumera, *Chem. Commun.* **2013**, *49*, 9125.
[18] X. Wang, C. Hu, L. Schurz, C. De Marco, X. Chen, S. Pané, B. J. Nelson, *ACS Nano* **2018**, *12*, 6210.
[19] S. Wang, L. Yang, H.-Y. Cho, S.-T. D. Chueng, H. Zhang, Q. Zhang, K.-B. Lee, *Biomaterials* **2019**, *224*, 119498.
[20] S. Khan, S. Setua, S. Kumari, N. Dan, A. Massey, B. B. Hafeez, M. M. Yallapu, Z. E. Stiles, A. Alabkaa, J. Yue, *Biomaterials* **2019**, *208*, 83.
[21] L. Zhang, Z. Liu, Y. Liu, Y. Wang, P. Tang, Y. Wu, H. Huang, Z. Gan, J. Liu, D. Wu, *Biomaterials* **2020**, *230*, 119655.
[22] E. Rahimi, R. Offoiach, S. Deng, X. Chen, S. Pané, L. Fedrizzi, M. Lekka, *Appl. Mater. Today* **2021**, *24*, 101135.
[23] E. Rahimi, R. Offoiach, K. Baert, H. Terryn, M. Lekka, L. Fedrizzi, *Materialia* **2021**, *15*, 100988.
[24] C. Zhang, W. Bu, D. Ni, S. Zhang, Q. Li, Z. Yao, J. Zhang, H. Yao, Z. Wang, J. Shi, *Angew. Chem.* **2016**, *128*, 2141.
[25] Y. S. Hedberg, *Npj Mater. Degrad.* **2018**, *2*, 26.
[26] H. Matusiewicz, *Acta Biomater.* **2014**, *10*, 2379.
[27] L. Vergara, M. Passeggi Jr, J. Ferron, *Appl. Surf. Sci.* **2002**, *187*, 199.
[28] D. Davies, W. Barker, *Corrosion* **1964**, *20*, 47t.
[29] W. Badawy, F. Al-Kharafi, J. Al-Ajmi, *J. Appl. Electrochem.* **2000**, *30*, 693.
[30] T. Maric, M. Z. M. Nasir, M. Budanovic, O. Alduhaish, R. D. Webster, M. Pumera, *Appl. Mater. Today* **2020**, *20*, 100659.
[31] X. Qian, J. Zhang, Z. Gu, Y. Chen, *Biomaterials* **2019**, *211*, 1.
[32] B. E.-F. de Ávila, P. Angsantikul, J. Li, M. Angel Lopez-Ramirez, D. E. Ramírez-Herrera, S. Thamphiwatana, C. Chen, J. Delezuk, R. Samakapiruk, V. Ramez, M. Obonyo, L. Zhang, J. Wang, *Nat. Commun.* **2017**, *8*, 272.
[33] C. Chen, X. Chang, P. Angsantikul, J. Li, B. Esteban-Fernández de Ávila, E. Karshalev, W. Liu, F. Mou, S. He, R. Castillo, *Adv. Biosyst.* **2018**, *2*, 1700160.
[34] Z. Wu, L. Li, Y. Yang, P. Hu, Y. Li, S.-Y. Yang, L. V. Wang, W. Gao, *Sci. Rob.* **2019**, *4*, eaax0613.
[35] J. Wang, Y. Dong, P. Ma, Y. Wang, F. Zhang, B. Cai, P. Chen, B. F. Liu, *Adv. Mater.* **2022**, *34*, 2201051.
[36] J. Llacer-Wintle, A. Rivas-Dapena, X.-Z. Chen, E. Pellicer, B. J. Nelson, J. Puigmartí-Luis, S. Pané, *Adv. Mater.* **2021**, *33*, 2102049.
[37] S. Wang, J. Xu, Q. Zhou, P. Geng, B. Wang, Y. Zhou, K. Liu, F. Peng, Y. Tu, *Adv. Healthcare Mater.* **2021**, *10*, 2100335.
[38] J. Li, J. Yu, *Nanomaterials* **2023**, *13*, 1590.
[39] S. Virtanen, I. Milošev, E. Gomez-Barrena, R. Trebše, J. Salo, Y. T. Konttinen, *Acta Biomater.* **2008**, *4*, 468.
[40] X. Meng, X. Zhang, M. Liu, B. Cai, N. He, Z. Wang, *Appl. Mater. Today* **2020**, *21*, 100864.
[41] Y. Liu, J. L. Gilbert, *J. Biomed. Mater. Res., Part B* **2018**, *106*, 209.
[42] J. Volatron, J. Kolosnjaj-Tabi, Y. Javed, Q. L. Vuong, Y. Gossuin, S. Neveu, N. Luciani, M. Hémadi, F. Carn, D. Alloyeau, *Sci. Rep.* **2017**, *7*, 40075.
[43] A. Balfourier, N. Luciani, G. Wang, G. Lelong, O. Ersen, A. Khelfa, D. Alloyeau, F. Gazeau, F. Carn, *Proc. Natl. Acad. Sci. USA* **2020**, *117*, 103.
[44] H. H. Jeong, M. Alarcón-Correa, A. G. Mark, K. Son, T. C. Lee, P. Fischer, *Adv. Sci.* **2017**, *4*, 1700234.
[45] Z. Liu, J. Zhang, P. Yu, J. Zhang, R. Makharia, K. More, E. Stach, *J. Electrochem. Soc.* **2010**, *157*, B906.
[46] J. I. Goldstein, D. E. Newbury, J. R. Michael, N. W. Ritchie, J. H. J. Scott, D. C. Joy, *Scanning Electron Microscopy and X-Ray Microanalysis*, Springer, Berlin **2017**.
[47] J. W. Olesik, *Anal. Chem.* **1991**, *63*, 12A.
[48] R. G. Kelly, J. R. Scully, D. Shoesmith, R. G. Buchheit, *Electrochemical Techniques in Corrosion Science and Engineering*, CRC Press, Boca Raton, FL **2002**.
[49] L. Liu, L. Zhang, S. M. Kim, S. Park, *Nanoscale* **2014**, *6*, 9355.
[50] A. Ghosh, D. Paria, G. Rangarajan, A. Ghosh, *J. Phys. Chem. Lett.* **2014**, *5*, 62.
[51] T. Li, J. Li, H. Zhang, X. Chang, W. Song, Y. Hu, G. Shao, E. Sandraz, G. Zhang, L. Li, J. Wang, *Small* **2016**, *12*, 6098.
[52] E. S. Olson, J. Orozco, Z. Wu, C. D. Malone, B. Yi, W. Gao, M. Eghtedari, J. Wang, R. F. Mattrey, *Biomaterials* **2013**, *34*, 8918.
[53] L. Ren, D. Zhou, Z. Mao, P. Xu, T. J. Huang, T. E. Mallouk, *ACS Nano* **2017**, *11*, 10591.
[54] S. Ahmed, W. Wang, L. Bai, D. T. Gentekos, M. Hoyos, T. E. Mallouk, *ACS Nano* **2016**, *10*, 4763.
[55] Y. Chen, B. Xu, Y. Mei, *Chem. Asian J.* **2019**, *14*, 2472.
[56] F. Wong, A. Sen, *ACS Nano* **2016**, *10*, 7172.
[57] D. Wang, C. Gao, W. Wang, M. Sun, B. Guo, H. Xie, Q. He, *ACS Nano* **2018**, *12*, 10212.
[58] C. C. Alcântara, S. Kim, S. Lee, B. Jang, P. Thakolkaran, J. Y. Kim, H. Choi, B. J. Nelson, S. Pané, *Small* **2019**, *15*, 1805006.
[59] Y. Yoshizumi, K. Okubo, M. Yokokawa, H. Suzuki, *Langmuir* **2016**, *32*, 9381.

[60] F. Mou, C. Chen, H. Ma, Y. Yin, Q. Wu, J. Guan, *Angew. Chem., Int. Ed.* **2013**, *52*, 7208.
[61] S. Wang, Z. Jiang, S. Ouyang, Z. Dai, T. Wang, *ACS Appl. Mater. Interfaces* **2017**, *9*, 23974.
[62] D. Ahmed, T. Baasch, B. Jang, S. Pane, J. Dual, B. J. Nelson, *Nano Lett.* **2016**, *16*, 4968.
[63] S. Schuerle, S. Pané, E. Pellicer, J. Sort, M. D. Baró, B. J. Nelson, *Small* **2012**, *8*, 1498.
[64] R. Liu, A. Sen, *J. Am. Chem. Soc.* **2011**, *133*, 20064.
[65] R. Jin, L. Liu, W. Zhu, D. Li, L. Yang, J. Duan, Z. Cai, Y. Nie, Y. Zhang, Q. Gong, *Biomaterials* **2019**, *203*, 23.
[66] H. Wang, G. Zhao, M. Pumera, *J. Am. Chem. Soc.* **2014**, *136*, 2719.
[67] X. Ma, S. Jang, M. N. Popescu, W. E. Uspal, A. Miguel-López, K. Hahn, D.-P. Kim, S. Sánchez, *ACS Nano* **2016**, *10*, 8751.
[68] N. Sanpo, C. C. Berndt, C. Wen, J. Wang, *Acta Biomater.* **2013**, *9*, 5830.
[69] D.b.R. Lima, N. Jiang, X. Liu, J. Wang, V. A. Vulcani, A. Martins, D. S. Machado, R. Landers, P. H. Camargo, A. Pancotti, *ACS Appl. Mater. Interfaces* **2017**, *9*, 39830.
[70] S. Novak, D. Drobne, M. Golobič, J. Zupanc, T. Romih, A. Gianoncelli, M. Kiskinova, B. Kaulich, P. Pelicon, P. Vavpetič, *Environ. Sci. Technol.* **2013**, *47*, 5400.
[71] Y. Okazaki, E. Gotoh, *Biomaterials* **2005**, *26*, 11.
[72] R. Narayan, *Biomedical Materials*, Springer, New York **2009**.
[73] L. Chang, Z. Zhifeng, L. Kwok-Yan, *Electrochim. Acta* **2017**, *241*, 331.
[74] W. Gao, A. Pei, J. Wang, *ACS Nano* **2012**, *6*, 8432.
[75] M. Hoop, F. Mushtaq, C. Hurter, X.-Z. Chen, B. J. Nelson, S. Pané, *Nanoscale* **2016**, *8*, 12723.
[76] F. Mushtaq, H. Torlakcik, M. Hoop, B. Jang, F. Carlson, T. Grunow, N. Läubli, A. Ferreira, X. Z. Chen, B. J. Nelson, *Adv. Funct. Mater.* **2019**, *29*, 1808135.
[77] D. D. Macdonald, A. Sun, *Electrochim. Acta* **2006**, *51*, 1767.
[78] Y. Liu, J. L. Gilbert, *Electrochim. Acta* **2018**, *262*, 252.
[79] G. S. Frankel, T. Li, J. R. Scully, *J. Electrochem. Soc.* **2017**, *164*, C180.
[80] E. McCafferty, *Introduction to Corrosion Science*, Springer, New York **2010**.
[81] W. Xu, F. Yu, L. Yang, B. Zhang, B. Hou, Y. Li, *Mater. Sci. Eng., C* **2018**, *92*, 11.
[82] E. Rahimi, A. Rafsanjani-Abbasi, A. Imani, A. Davoodi, *Mater. Chem. Phys.* **2018**, *212*, 403.
[83] M. Rohwerder, F. Turcu, *Electrochim. Acta* **2007**, *53*, 290.
[84] E. Rahimi, A. Rafsanjani-Abbasi, A. Imani, S. Hosseinpour, A. Davoodi, *Corros. Sci.* **2018**, *140*, 30.
[85] Z. Esfahani, E. Rahimi, M. Sarvghad, A. Rafsanjani-Abbasi, A. Davoodi, *J. Alloys Compd.* **2018**, *744*, 174.
[86] K. Kim, J. Guo, X. Xu, D. Fan, *ACS Nano* **2015**, *9*, 548.
[87] H. B. Michaelson, *J. Appl. Phys.* **1977**, *48*, 4729.
[88] M. T. Greiner, Z.-H. Lu, *NPG Asia Mater.* **2013**, *5*, 55.
[89] E. Rahimi, A. Kosari, S. Hosseinpour, A. Davoodi, H. Zandbergen, J. M. Mol, *Appl. Surf. Sci.* **2019**, *496*, 143634.
[90] E. Rahimi, A. Rafsanjani-Abbasi, A. Davoodi, S. Hosseinpour, *J. Electrochem. Soc.* **2019**, *166*, C609.
[91] A. Mellado-Valero, A. I. Muñoz, V. G. Pina, M. F. Sola-Ruiz, *Materials* **2018**, *11*, 171.
[92] J. Li, P. Angsantikul, W. Liu, B. Esteban-Fernández de Ávila, S. Thamphiwatana, M. Xu, E. Sandraz, X. Wang, J. Delezuk, W. Gao, L. Zhang, J. Wang, *Angew. Chem., Int. Ed.* **2017**, *56*, 2156.
[93] C. K. Schmidt, M. Medina-Sánchez, R. J. Edmondson, O. G. Schmidt, *Nat. Commun.* **2020**, *11*, 5618.
[94] X.-Z. Chen, M. Hoop, F. Mushtaq, E. Siringil, C. Hu, B. J. Nelson, S. Pané, *Appl. Mater. Today* **2017**, *9*, 37.
[95] A. E. Nel, L. Mädler, D. Velegol, T. Xia, E. M. Hoek, P. Somasundaran, F. Klaessig, V. Castranova, M. Thompson, *Nat. Mater.* **2009**, *8*, 543.
[96] J. Wang, Z. Xiong, J. Zheng, X. Zhan, J. Tang, *Acc. Chem. Res.* **2018**, *51*, 1957.
[97] T. Patiño, X. Arqué, R. Mestre, L. Palacios, S. Sánchez, *Acc. Chem. Res.* **2018**, *51*, 2662.
[98] K. K. Dey, A. Sen, *J. Am. Chem. Soc.* **2017**, *139*, 7666.
[99] E. Rahimi, A. Rafsanjani-Abbasi, A. Kiani-Rashid, H. Jafari, A. Davoodi, *Colloids Surf. A* **2018**, *547*, 81.
[100] U. Choudhury, L. Soler, J. G. Gibbs, S. Sanchez, P. Fischer, *Chem. Commun.* **2015**, *51*, 8660.
[101] S. Wang, N. Wu, *Langmuir* **2014**, *30*, 3477.
[102] M. Safdar, T. D. Minh, N. Kinnunen, J. Jänis, *ACS Appl. Mater. Interfaces* **2016**, *8*, 32624.
[103] C. Gao, C. Zhou, Z. Lin, M. Yang, Q. He, *ACS Nano* **2019**, *13*, 12758.
[104] W. Wang, T.-Y. Chiang, D. Velegol, T. E. Mallouk, *J. Am. Chem. Soc.* **2013**, *135*, 10557.
[105] Y. Hong, M. Diaz, U. M. Córdova-Figueroa, A. Sen, *Adv. Funct. Mater.* **2010**, *20*, 1568.
[106] M. Luo, Y. Jiang, J. Su, Z. Deng, F. Mou, L. Xu, J. Guan, *Chem. Asian J.* **2019**, *14*, 2503.
[107] M. Talha, Y. Ma, P. Kumar, Y. Lin, A. Singh, *Colloids Surf., B* **2019**, *176*, 494.
[108] S. Karimi, T. Nickchi, A. Alfantazi, *Corros. Sci.* **2011**, *53*, 3262.
[109] S. Takemoto, M. Hattori, M. Yoshinari, E. Kawada, Y. Oda, *Biomaterials* **2005**, *26*, 829.
[110] I. Milošev, in *Biomedical Applications*, (Ed: S. S. Djokić), Springer, New York **2012**, pp. 1–72.
[111] Z. B. Wang, H. X. Hu, Y. G. Zheng, *Corros. Sci.* **2018**, *130*, 203.
[112] P. L. Venugopalan, R. Sai, Y. Chandorkar, B. Basu, S. Shivashankar, A. Ghosh, *Nano Lett.* **2014**, *14*, 1968.
[113] Z. Wu, Y. Chen, D. Mukasa, O. S. Pak, W. Gao, *Chem. Soc. Rev.* **2020**, *49*, 8088.
[114] I. Milošev, *Electrochim. Acta* **2012**, *78*, 259.
[115] T. Guckeisen, S. Hosseinpour, W. Peukert, *Langmuir* **2019**, *35*, 5004.
[116] H. Willert, L. Brobäck, G. Buchhorn, P. Jensen, G. Köster, I. Lang, P. Ochsner, R. Schenk, *Clin. Orthop. Relat. Res.* **1996**, *333*, 51.
[117] W. Gao, A. Uygun, J. Wang, *J. Am. Chem. Soc.* **2012**, *134*, 897.
[118] R. Tsaryk, M. Kalbacova, U. Hempel, D. Scharnweber, R. E. Unger, P. Dieter, C. J. Kirkpatrick, K. Peters, *Biomaterials* **2007**, *28*, 806.
[119] T. Kocha, M. Yamaguchi, H. Ohtaki, T. Fukuda, T. Aoyagi, *Biochim. Biophys. Acta* **1997**, *1337*, 319.
[120] Y. Zhang, O. Addison, F. Yu, B. C. R. Troconis, J. R. Scully, A. J. Davenport, *Sci. Rep.* **2018**, *8*, 3185.
[121] T. Maric, M. Z. M. Nasir, Y. Wang, B. Khezri, M. Pumera, *Nanoscale* **2018**, *10*, 1322.
[122] M. Bobu, A. Yediler, I. Siminiceanu, S. Schulte-Hostede, *Appl. Catal., B* **2008**, *83*, 15.
[123] M. F. Yoder, W. S. Kisaalita, *J. Biol. Eng.* **2011**, *5*, 4.
[124] N. E. Putra, M. A. Leeflang, M. Minneboo, P. Taheri, L. E. Fratila-Apachitei, J. M. C. Mol, J. Zhou, A. A. Zadpoor, *Acta Biomater.* **2021**, *121*, 741.
[125] Z. Zhou, D. Huang, J. Bao, Q. Chen, G. Liu, Z. Chen, X. Chen, J. Gao, *Adv. Mater.* **2012**, *24*, 6223.
[126] M. C. Hohnholt, M. Geppert, R. Dringen, *Acta Biomater.* **2011**, *7*, 3946.
[127] C. C. Winterbourn, *Toxicol. Lett.* **1995**, *82*, 969.
[128] M. L. Kremer, *J. Phys. Chem. A* **2003**, *107*, 1734.
[129] D. Arndt, T. M. Gesing, M. Bäumer, *ChemPlusChem* **2012**, *77*, 576.
[130] R. J. Wydra, P. G. Rychahou, B. M. Evers, K. W. Anderson, T. D. Dziubla, J. Z. Hilt, *Acta Biomater.* **2015**, *25*, 284.
[131] Y. Dai, Z. Yang, S. Cheng, Z. Wang, R. Zhang, G. Zhu, Z. Wang, B. C. Yung, R. Tian, O. Jacobson, *Adv. Mater.* **2018**, *30*, 1704877.
[132] W. K. Ong, X. Yao, D. Jana, M. Li, Y. Zhao, Z. Luo, *Small Struct.* **2020**, *1*, 2000065.
[133] Z. Tang, Y. Liu, M. He, W. Bu, *Angew. Chem., Int. Ed.* **2019**, *58*, 946.

[134] Y. Yan, H. Yang, Y. Su, L. Qiao, *Sci. Rep.* **2015**, *5*, 18403.
[135] M. Talha, Y. Ma, P. Kumar, Y. Lin, A. Singh, *Colloids Surf., B* **2019**, *176*, 494.
[136] Y. Li, K. G. Neoh, E.-T. Kang, *J. Colloid Interface Sci.* **2004**, *275*, 488.
[137] M. L. W. Knetsch, Y. B. J. Aldenhoff, L. H. Koole, *Biomaterials* **2006**, *27*, 2813.
[138] C. V. Vidal, A. I. Muñoz, *Electrochim. Acta* **2010**, *55*, 8445.
[139] S. H. Teoh, *Engineering Materials for Biomedical Applications*, World Scientific, Singapore **2004**.
[140] K. Villa, J. Viktorova, J. Plutnar, T. Ruml, L. Hoang, M. Pumera, *Cell Rep. Phys. Sci.* **2020**, *1*, 100181.
[141] J. Mosquera, I. García, M. Henriksen-Lacey, M. Martínez-Calvo, M. Dhanjani, J. L. Mascareñas, L. M. Liz-Marzán, *ACS Nano* **2020**, *14*, 5382.
[142] J. Kolosnjaj-Tabi, Y. Javed, L. Lartigue, J. Volatron, D. Elgrabli, I. Marangon, G. Pugliese, B. Caron, A. Figuerola, N. Luciani, *ACS Nano* **2015**, *9*, 7925.
[143] W. He, J. Frueh, N. Hu, L. Liu, M. Gai, Q. He, *Adv. Sci.* **2016**, *3*, 1600206.
[144] E. Karshalev, Y. Zhang, B. Esteban-Fernández de Ávila, M. Beltrán-Gastélum, Y. Chen, R. Mundaca-Uribe, F. Zhang, B. Nguyen, Y. Tong, R. H. Fang, L. Zhang, J. Wang, *Nano Lett.* **2019**, *19*, 7816.
[145] S. P. H. Moghaddam, R. Mohammadpour, H. Ghandehari, *J. Controlled Release* **2019**, *311*, 1.
[146] A. Laskar, M. Ghosh, S. I. Khattak, W. Li, X.-M. Yuan, *Nanomedicine* **2012**, *7*, 705.
[147] V. De Matteis, M. Cascione, V. Brunetti, C. C. Toma, R. Rinaldi, *Toxicol. In Vitro* **2016**, *37*, 201.
[148] A. Van de Walle, J. Kolosnjaj-Tabi, Y. Lalatonne, C. Wilhelm, *Acc. Chem. Res.* **2020**, *53*, 2212.
[149] J. Kolosnjaj-Tabi, L. Lartigue, Y. Javed, N. Luciani, T. Pellegrino, C. Wilhelm, D. Alloyeau, F. Gazeau, *Nano Today* **2016**, *11*, 280.
[150] S. J. Soenen, J.-M. Montenegro, A. M. Abdelmonem, B. B. Manshian, S. H. Doak, W. J. Parak, S. C. De Smedt, K. Braeckmans, *Acta Biomater.* **2014**, *10*, 732.
[151] J. Volatron, F. Carn, J. Kolosnjaj-Tabi, Y. Javed, Q. L. Vuong, Y. Gossuin, C. Ménager, N. Luciani, G. Charron, M. Hémadi, *Small* **2017**, *13*, 1602030.
[152] M. Safi, M. Yan, M.-A. Guedeau-Boudeville, H. Conjeaud, V. Garnier-Thibaud, N. Boggetto, A. Baeza-Squiban, F. Niedergang, D. Averbeck, J.-F. Berret, *ACS Nano* **2011**, *5*, 5354.
[153] M. Levy, N. Luciani, D. Alloyeau, D. Elgrabli, V. Deveaux, C. Pechoux, S. Chat, G. Wang, N. Vats, F. Gendron, *Biomaterials* **2011**, *32*, 3988.
[154] M. Pal, N. Somalwar, A. Singh, R. Bhat, S. M. Eswarappa, D. K. Saini, A. Ghosh, *Adv. Mater.* **2018**, *30*, 1800429.
[155] V. M. Kadiri, C. Bussi, A. W. Holle, K. Son, H. Kwon, G. Schütz, M. G. Gutierrez, P. Fischer, *Adv. Mater.* **2020**, *32*, 2001114.
[156] R. Ghosh Chaudhuri, S. Paria, *Chem. Rev.* **2012**, *112*, 2373.
[157] M. B. Gawande, A. Goswami, T. Asefa, H. Guo, A. V. Biradar, D.-L. Peng, R. Zboril, R. S. Varma, *Chem. Soc. Rev.* **2015**, *44*, 7540.
[158] M. N. Nadagouda, R. S. Varma, *Cryst Growth Des.* **2007**, *7*, 2582.
[159] D. Ling, T. Hyeon, *Small* **2013**, *9*, 1450.
[160] W.-r. Lee, M. G. Kim, J.-r. Choi, J.-I. Park, S. J. Ko, S. J. Oh, J. Cheon, *J. Am. Chem. Soc.* **2005**, *127*, 16090.
[161] L. Lu, W. Zhang, D. Wang, X. Xu, J. Miao, Y. Jiang, *Mater. Lett.* **2010**, *64*, 1732.
[162] R. Mardosaitė, A. Jurkevičiūtė, S. Račkauskas, *Cryst. Growth Des.* **2021**, *21*, 4765.
[163] Y. Qin, Y. Kim, L. Zhang, S. M. Lee, R. B. Yang, A. Pan, K. Mathwig, M. Alexe, U. Gösele, M. Knez, *Small* **2010**, *6*, 910.
[164] X. Han, Y. Liu, Z. Jia, Y.-C. Chen, J. Wan, N. Weadock, K. J. Gaskell, T. Li, L. Hu, *Nano Lett.* **2014**, *14*, 139.
[165] M. Knez, R. Scholz, K. Nielsch, E. Pippel, D. Hesse, M. Zacharias, U. Gösele, *Nat. Mater.* **2006**, *5*, 627.
[166] I. Spajić, E. Rahimi, M. Lekka, R. Offoiach, L. Fedrizzi, I. Milošev, *J. Electrochem. Soc.* **2021**, *168*, 071510.
[167] L. F. Hakim, C. L. Vaughn, H. J. Dunsheath, C. S. Carney, X. Liang, P. Li, A. W. Weimer, *Nanotechnology* **2007**, *18*, 345603.
[168] J. A. McCormick, K. P. Rice, D. F. Paul, A. W. Weimer, S. M. George, *Chem. Vap. Deposition* **2007**, *13*, 491.
[169] S. Schuerle, I. A. Vizcarra, J. Moeller, M. S. Sakar, B. Özkale, A. M. Lindo, F. Mushtaq, I. Schoen, S. Pané, V. Vogel, *Sci Robot* **2017**, *2*, eaah6094.
[170] V. Georgiadou, G. Makris, D. Papagiannopoulou, G. Vourlias, C. Dendrinou-Samara, *ACS Appl. Mater. Interfaces* **2016**, *8*, 9345.
[171] R. N. Grass, E. K. Athanassiou, W. J. Stark, *Angew. Chem., Int. Ed.* **2007**, *46*, 4909.
[172] P. Del Pino, B. Pelaz, Q. Zhang, P. Maffre, G. U. Nienhaus, W. J. Parak, *Mater. Horiz.* **2014**, *1*, 301.
[173] C. D. Walkey, W. C. Chan, *Chem. Soc. Rev.* **2012**, *41*, 2780.
[174] G. Stepien, M. Moros, M. Pérez-Hernández, M. Monge, L. Gutiérrez, R. M. Fratila, M.d. Heras, S. M. Guillen, J. J. P. Lanzarote, C. Solans, *ACS Appl. Mater. Interfaces* **2018**, *10*, 4548.
[175] C. Fang, N. Bhattarai, C. Sun, M. Zhang, *Small* **2009**, *5*, 1637.
[176] V. H. Ho, K. H. Müller, A. Barcza, R. Chen, N. K. Slater, *Biomaterials* **2010**, *31*, 3095.
[177] M. Muthana, S. D. Scott, N. Farrow, F. Morrow, C. Murdoch, S. Grubb, N. Brown, J. Dobson, C. Lewis, *Gene Ther.* **2008**, *15*, 902.
[178] T. R. Pisanic II, J. D. Blackwell, V. I. Shubayev, R. R. Fiñones, S. Jin, *Biomaterials* **2007**, *28*, 2572.
[179] B. Mattix, T. R. Olsen, T. Moore, M. Casco, D. Simionescu, R. P. Visconti, F. Alexis, *Adv. Funct. Mater.* **2014**, *24*, 800.
[180] G. Gąsior, J. Szczepański, A. Radtke, *Materials* **2021**, *14*, 3381.
[181] M. Asgari, R. Hang, C. Wang, Z. Yu, Z. Li, Y. Xiao, *Metals* **2018**, *8*, 212.
[182] H. Hermawan, D. Dubé, D. Mantovani, *J. Biomed. Mater. Res. A* **2010**, *93*, 1.
[183] B. Jang, E. Gutman, N. Stucki, B. F. Seitz, P. D. Wendel-García, T. Newton, J. Pokki, O. Ergeneman, S. Pané, Y. Or, *Nano Lett.* **2015**, *15*, 4829.
[184] T.-Y. Huang, F. Qiu, H.-W. Tung, X.-B. Chen, B. J. Nelson, M. S. Sakar, *Appl. Phys. Lett.* **2014**, *105*, 114102.
[185] W. Liu, H. Ge, X. Ding, X. Lu, Y. Zhang, Z. Gu, *Nanoscale* **2020**, *12*, 19655.
[186] S. M. Beladi-Mousavi, B. Khezri, L. Krejčová, Z.k. Heger, Z.k. Sofer, A. C. Fisher, M. Pumera, *ACS Appl. Mater. Interfaces* **2019**, *11*, 13359.
[187] H. Wang, J. G. S. Moo, M. Pumera, *ACS Nano* **2016**, *10*, 5041.
[188] M. A. Zeeshan, S. Pané, S. K. Youn, E. Pellicer, S. Schuerle, J. Sort, S. Fusco, A. M. Lindo, H. G. Park, B. J. Nelson, *Adv. Funct. Mater.* **2013**, *23*, 823.
[189] B. Jang, E. Pellicer, M. Guerrero, X. Chen, H. Choi, B. J. Nelson, J. Sort, S. Pané, *ACS Appl. Mater. Interfaces* **2014**, *6*, 14583.
[190] F. M. Kievit, Z. R. Stephen, K. Wang, C. J. Dayringer, J. G. Sham, R. G. Ellenbogen, J. R. Silber, M. Zhang, *Mol. Oncol.* **2015**, *9*, 1071.
[191] D. Kim, M. K. Yu, T. S. Lee, J. J. Park, Y. Y. Jeong, S. Jon, *Nanotechnology* **2011**, *22*, 155101.
[192] A. Espinosa, A. Curcio, S. Cabana, G. Radtke, M. Bugnet, J. Kolosnjaj-Tabi, C. Péchoux, C. Alvarez-Lorenzo, G. A. Botton, A. K. Silva, *ACS Nano* **2018**, *12*, 6523.
[193] M. Geppert, M. C. Hohnholt, S. Nürnberger, R. Dringen, *Acta Biomater.* **2012**, *8*, 3832.
[194] A. Van de Walle, A. P. Sangnier, A. Abou-Hassan, A. Curcio, M. Hemadi, N. Menguy, Y. Lalatonne, N. Luciani, C. Wilhelm, *Proc. Natl. Acad. Sci. USA* **2019**, *116*, 4044.
[195] S. Nizamov, O. Kasian, V. M. Mirsky, *Angew. Chem., Int. Ed.* **2016**, *55*, 7247.

Ehsan Rahimi obtained his Ph.D. (October 2021) entitled "Localized Corrosion Mechanism on Micro- and Nano Devices in Biomedical Field" in environmental and energy engineering science at the University of Udine. As part of his Marie Curie Ph.D. project, he visited Multi-Scale Robotics Lab of the Institute of Robotics and Intelligent Systems at ETH Zürich (June 2019) focusing on the biodegradation mechanisms of micro and nanorobotic platforms. In May 2022, he joined the corrosion technology and electrochemistry group at Delft University of Technology as a postdoctoral researcher working on advanced measuring/modelling of corrosion processes in industrial areas to energy and biomaterials sciences.

Roger Sanchis Gual obtained his B.Sc. in chemistry at the University of Valencia and his MSc in electrochemistry at the University of Cordoba. From 2016 to 2021, he pursued his Ph.D. in nanoscience and nanotechnology at the University of Valencia, supported by a prestigious Spanish fellowship. During this time, he combined colloidal chemistry with coordination chemistry to design hybrid nanomaterials with improved magnetic, electric and electrochemical properties. In 2022, he joined the Multi-Scale Robotics Lab at ETH Zurich as a postdoctoral associate. His current research focuses on developing magnetic and biodegradable microrobots for biomedical applications.

Salvador Pané is professor of materials for robotics and co-director of the Multi-Scale Robotics Lab (MSRL) at ETH Zürich. He received his Ph.D. in chemistry from the University of Barcelona in 2008 and subsequently joined MSRL as a postdoctoral researcher in August 2008. He was awarded the highly competitive ERC-StG and ERC-CoG in 2012 and 2017, respectively. His interests lie in bridging materials science, chemistry, and electrochemistry with small-scale robotics for various applications.

Maria Lekka is the head of the coatings and surface treatments unit of CIDETEC Surface Engineering at San Sebastian, Spain. She obtained her master's degree in chemical engineering at National Technical University of Athens (Greece) in 2003 and her Ph.D. in materials engineering and industrial technologies at University of Trento (Italy) in 2008. Her main research activities focus on the research and development of innovative coatings for corrosion and wear protection by chemical and electrochemical processes as well as in the study of corrosion mechanisms by localized electrochemical techniques.